

Control/physical systems co-design with spectral temporal logic specifications and its applications to MEMS

Gang Chen, Zhaodan Kong & Longhan Xie

To cite this article: Gang Chen, Zhaodan Kong & Longhan Xie (31 Jan 2024): Control/physical systems co-design with spectral temporal logic specifications and its applications to MEMS, International Journal of Control, DOI: [10.1080/00207179.2024.2310610](https://doi.org/10.1080/00207179.2024.2310610)

To link to this article: <https://doi.org/10.1080/00207179.2024.2310610>



Published online: 31 Jan 2024.



Submit your article to this journal [↗](#)



View related articles [↗](#)



View Crossmark data [↗](#)



Control/physical systems co-design with spectral temporal logic specifications and its applications to MEMS

Gang Chen^a, Zhaodan Kong^b and Longhan Xie^a

^aShien-Ming Wu School of Intelligent Engineering, South China University of Technology, Guangzhou, People's Republic of China; ^bDepartment of Mechanical & Aerospace Engineering, University of California Davis, Davis, CA, USA

ABSTRACT

'Co-design' problems try to simultaneously design the physical and control components to improve the overall system performance. However, existing co-design paradigms cannot deal with complex frequency temporal domain specifications. In this paper, we investigate the co-design problem for a class of linear parameter-varying (LPV) systems with frequency temporal domain specifications. Firstly, the frequency temporal domain specifications are written in a formal language called spectral temporal logic (STL). Secondly, the satisfaction conditions of the spectral temporal logic specifications have been transformed into non-linear matrices inequality forms with necessary and sufficient conditions. Thirdly, the co-design problem is transformed into a non-convex optimisation problem with mixed-integer linear matrix inequalities (MILMIs) constraints, and then an iterative algorithm is proposed to solve the co-design problem with semidefinite programming (SDP). Finally, the performance of the algorithm and the expressiveness of spectral temporal logic are illustrated with the applications to micro-electromechanical systems (MEMS).

ARTICLE HISTORY

Received 16 September 2022
Accepted 22 January 2024

KEYWORDS

Co-design;
micro-electromechanical systems; spectral temporal logic; mixed-integer linear matrix inequality

1. Introduction

The development of closed-loop controlled dynamic systems often employs a troublesome serial arrangement of tasks, wherein physical design parameters are settled first, and then the control parameters are computed to satisfy some desired specifications. As a result of the interdependence between control and physical parameters through system dynamics (Skelton, 1989), the design of a physical system and its controller in this often decoupled fashion can present formidable problems in practice, e.g. the efficiency requirements of piezoelectric optomechanical platforms can not be satisfied (Balram & Srinivasan, 2022). Completing these tasks simultaneously will significantly improve the overall system performance (Silvas et al., 2017): a process called 'co-design' (Allison et al., 2014).

Co-design has been studied in the literature under names such as 'integrated physical system and control design' and is widely applicable to almost every engineering field. A variety of strategies have been proposed to solve the co-design problem (Chanekar et al., 2016). Specifically, for linear dynamic systems, the co-design problems in the existing literature have been transformed into non-convex optimisation problems with non-convex constraints and convex objective functions. The non-convex constraints come from the Algebraic Riccati Equation (ARE) constraints, which usually have a bilinear matrix inequality (BMI) form Chiu (2017). Several methods to address the BMI conditions have been well established, and a brief overview of these methods can be found in Chanekar et al. (2018). However, to the best of our knowledge, few studies have investigated the co-design problem with frequency temporal domain

specifications, in which the system should satisfy system stability conditions and desired spectral temporal domain specifications simultaneously.

The need of co-design with frequency domain specifications has been discussed in many fields, such as MEMS-based quantum microwave-to-optical signal transduction (Balram & Srinivasan, 2022), cyber-physical systems (Rizzon & Passerone, 2016), and CMOS radio frequency energy harvesters (Karami & Moez, 2019). Most MEMS devices are designed to operate at their mechanical resonance frequency and co-design with frequency domain specifications for these resonant-based MEMS devices involves two major challenges. The first challenge is the non-BMI constraints induced by the frequency domain specifications in the form of frequency domain inequality (FDI). To solve the control synthesis problems with FDI, the generalised KYP (GKYP) (Iwasaki & Hara, 2005) lemma has been widely used to convert FDI to linear matrix inequalities (LMIs). Specifically, given a frequency domain specification defined by matrices $\Psi, \Phi \in \mathbb{H}_2$ that define a frequency range (See Definition 2.2), the GKYP lemma implies that the system is asymptotically stable and satisfies the specification if and only if there exist Hermitian matrices P, Q , and $Q > 0$, such that the following inequality

$$\begin{bmatrix} \mathbf{A} & \mathbf{B} \\ \mathbf{I} & 0 \end{bmatrix}^T [\Phi \otimes P + \Psi \otimes Q] \begin{bmatrix} \mathbf{A} & \mathbf{B} \\ \mathbf{I} & 0 \end{bmatrix} + \Lambda < 0 \quad (1)$$

is satisfied, where $\Lambda = \begin{bmatrix} \mathbf{C} & \mathbf{D} \\ 0 & \mathbf{I} \end{bmatrix}^T \Pi \begin{bmatrix} \mathbf{C} & \mathbf{D} \\ 0 & \mathbf{I} \end{bmatrix}$ and $\mathbf{A}, \mathbf{B}, \mathbf{C}, \mathbf{D}$ are the closed-loop system matrices of a linear time-invariant (LTI)

system, which include physical and control parameters. If we assume the physical parameters are fixed, the constraints in (1) can be transformed into a sequence of LMIs based on the results in Li and Gao (2014). However, when we take the physical parameters into consideration, the stability condition defined in (1) involves a different type of non-convexity and cannot be transformed into LMIs with existing methods. Obviously, the condition for the satisfaction of frequency domain specifications is no longer BMIs. Therefore, the problem of control/physical *co-design* subject to frequency domain specifications for a linear system is still open and a challenge.

Alongside the challenge of non-BMI form for stability conditions, many resonant-type devices do not work under fixed-frequency scenarios and the excitation frequencies for these devices have complex high-level temporal patterns. This is a challenge to describe these high-level patterns with FDIs. For example, for the frequency excitation systems (Ilyas et al., 2017a) and frequency monitoring system (Zhong et al., 2005), the solving of the co-design problem should address procedure frequency domain specifications, which should satisfy some temporal frequency events that have high-level logic patterns. For example, the MEMS logic devices in Ilyas et al. (2017a, 2017b) can perform the fundamental logic gate AND, OR, and universal logic gates NAND, NOR, by exciting combination resonances, which requires the frequency response of the systems to have temporal logic patterns, i.e. the combination of multi-frequency domain specifications in temporal logic form. A spectral temporal specification for a logic device can be

the system's frequency response should be always smaller than 0.3 within $[1, 100]$ rad/s to realise logic gate "AND", and if logic AND has been performed, then the frequency response should be eventually larger than 1 with in $[100, 120]$ rad/s to realise logic OR in the next 5 millisecond.

In general, the spectral temporal properties of a given system's performance are commonly exchanged between industrial organisations for the purposes of requirement-setting in the design of highly-integrated products. In that context, a supplier might be required to simultaneously meet spectral and temporal domain specifications on, e.g. resonance peaks, effective bandwidths, steady-state behaviour, and quality factor, under multiple external forcing conditions. Reasoning about these complex spectral requirements should employ the same principled and formal constructs as temporal analyses of these measured or predicted traces, while FDI-based specification cannot meet this demand for complex spectral temporal reasoning. Therefore, existing studies about codesign with spectral temporal domain specifications demand further investigation.

To address the aforementioned issues, the spectral temporal domain specifications for the co-design problem are described with a novel logic, called spectral temporal logic (STL) in this paper. STL is inspired by signal temporal logic, which was introduced in Maler and Nickovic (2004) to specify continuous-time real signals and since then has been widely used in the verification, analysis and synthesis of cyber-physical systems (Chen et al., 2018). STL is expressive in terms of describing multiple frequency temporal domain specifications in complex patterns, e.g. combining spectral specifications with 'AND' or 'OR' operators along temporal domain. STL enables transforming multiple

spectral domain specifications, combined in multiple forms, into MILMIs. It is also equipped with a quantitative semantic, called robustness degree, which measures to what extent a system satisfies or does not satisfy a given spectral temporal domain specification. In summary, the contributions of this paper are twofold.

- *Formalism*: we propose a spectral temporal logic, which is the first formal language (to the best of our knowledge) specifically for characterising and reasoning about spectral temporal domain specifications. Moreover, a generalised STL lemma is derived to check whether a system satisfies STL specifications.
- *Algorithm*: we develop a novel and systematic iterative algorithm to solve the co-design problem for a class of discrete-time LPV systems with specifications defined by STL formulas. To eliminate the non-convex constraints imposed by the frequency temporal domain specifications, we derive some theorems to transform the non-convex constraints into convex ones.

This paper is organised as follows: Section 2 defines the concept of spectral temporal logic. Section 3 formulates the co-design problem solved in this paper. Section 4 solves the problem with an iterative algorithm, with some theoretical results provided to guarantee the performance. Section 5 validates the proposed method with numerical examples, and our conclusions are summarised in Section 6.

Notations: The superscripts -1 , T , $*$ stand for inverse, transpose, and conjugate transpose of a matrix, respectively. $\mathbb{R}^{m \times n}$ and $\mathbb{C}^{m \times n}$ are the set of all $m \times n$ real and complex matrices, respectively. \mathbb{H}_n and \mathbb{S}_n stand for the set of $n \times n$ Hermitian and symmetric matrices, respectively. \mathbf{I} denotes an identity matrix with appropriate dimension. $\text{sym}\{A\} = A^T + A$. For $M \in \mathbb{H}_n$, inequalities $M > (\geq) 0$ and $M < (\leq) 0$ denote positive (semi) definiteness and negative (semi) definiteness, respectively. $\Phi \otimes P$ means the Kronecker product of matrices Φ and P . $\Re(A)$ and $\Im(A)$ denote the real and imaginary part of matrix A .

2. Spectral temporal logic specifications

In this section, we will first propose and define the syntax and semantics of a new logic called *spectral temporal logic*. We then will provide some nice properties of STL, particularly in the context of LPV systems.

Definition 2.1 (STL Syntax): Given a set of matrices $G(e^{j\omega}, t) \in \mathbb{C}^{n \times m}$ parameterised by ω and t , which is defined over a continuous frequency range $[\omega_1, \omega_2]$ and a discrete time range $[a, b]$, an STL formula φ is recursively defined as,

$$\begin{aligned} \psi &:= \psi_1 \vee \psi_2 | \psi_1 \wedge \psi_2 | \square_{[\omega_1, \omega_2]} \mu | \diamond_{[\omega_1, \omega_2]} \mu, \\ \varphi &:= \psi | \varphi_1 \wedge \varphi_2 | \varphi_1 \vee \varphi_2 | \square_{[a, b]} \psi | \boxplus_{[a, b]} \psi \end{aligned} \quad (2)$$

where $\mu \in \Delta$ is a predicate in the form $\mu := f(G(e^{j\omega}, t), \Pi) < 0$, with $f : \mathbb{C}^{n \times m} \times \mathbb{H}_{n+m} \rightarrow \mathbb{H}_m$ defined by

$$f(G, \Pi) := \begin{bmatrix} G \\ \mathbf{I}_m \end{bmatrix}^* \Pi \begin{bmatrix} G \\ \mathbf{I}_m \end{bmatrix}. \quad (3)$$

Additionally, $\Pi \in \mathbb{H}_{n+m}$, \wedge and \vee are conjunction and disjunction connectives, respectively; \mathbf{I}_m is an identity matrix with dimension $m \times m$; and \diamond , \square , \boxminus , and \boxplus are the operators denoting ‘eventually’, ‘always’, for spectral specifications, and ‘always’, ‘eventually’, for temporal specifications, respectively. Given a system G and STL formula φ , $G(e^{j\omega}, t) \models \varphi$ denotes the system $G(e^{j\omega}, t)$ satisfies formula φ at time t .

Remark 2.1: The syntax of STL is inspired by signal temporal logic (Raman et al., 2014) defined over the frequency response curve of a parametric varying system defined by matrix $G(e^{j\omega}, t)$. One argument of f is a Hermitian matrix Π , which is a user-defined matrix and can be conveniently used to specify bounds on $G(e^{j\omega}, t)$. Assume that predicate μ requires that $G(e^{j\omega}, t)$ is bounded, e.g. setting matrix $\Pi = \text{diag}\{\mathbf{I}, -\eta^2\mathbf{I}\}$ of μ leads to $\|G(e^{j\omega}, t)\|_\infty < \eta$, and predicate μ' requires that $G(e^{j\omega}, t)$ should be larger than a value, e.g. setting matrix $\Pi = \text{diag}\{-\mathbf{I}, \eta^2\mathbf{I}\}$ of μ' leads to $\|G(e^{j\omega}, t)\|_\infty \geq \eta$. $\psi_1 \wedge \psi_2$ denotes $G(e^{j\omega}, t)$ should satisfy specification ψ_1 and ψ_2 simultaneously. $\psi_1 \vee \psi_2$ denotes $G(e^{j\omega}, t)$ should satisfy specification ψ_1 or ψ_2 . $\square_{[\omega_1, \omega_2]}\psi$ denotes $G(e^{j\omega}, t)$ should satisfy specification ψ within frequency range $[\omega_1, \omega_2]$ and $\diamond_{[\omega_1, \omega_2]}\mu$ denotes the value for $G(e^{j\omega}, t)$ should be larger or smaller than a threshold at least once within frequency range $[\omega_1, \omega_2]$. Note that the formula φ allows nesting operators, e.g. formulas with form $\square_{[a, b]}\diamond_{[\omega_1, \omega_2]}\mu$ are allowed, and the first operator is defined on discrete time range.

STL is expressiveness in defining spectral temporal specifications along time domain. Consider the case where $G(e^{j\omega}, t)$ is a single-input-single-output (SISO) transfer function and the satisfiable $G(e^{j\omega}, t)$ is a general conic section on the complex plane, denoted as Ξ , which can be characterised by

$$\Xi = \left\{ G(e^{j\omega}, t) \in \mathbb{C} : G(e^{j\omega}, t) := \begin{bmatrix} \Re(G(e^{j\omega}, t)) \\ \Im(G(e^{j\omega}, t)) \end{bmatrix}, \right. \\ \left. f(G(e^{j\omega}, t), \Pi) < 0 \right\} \quad (4)$$

Based on the results in Iwasaki and Hara (2005), let a real matrix $\Delta \in \mathbb{H}_3$ be given and consider the set Ξ in (4), the matrix Δ can be partitioned as

$$\begin{bmatrix} W_\delta & q \\ q^T & r \end{bmatrix} := \Delta, \quad W_\delta = W_\delta^T = U_\delta t U_\delta^T, \quad q \in \mathbb{R}^2, \quad R \in \mathbb{R} \quad (5)$$

where $U_\delta U_\delta^T = \mathbf{I}$ and $t = \text{diag}(\zeta_1, \zeta_2)$. Then the set Ξ has an interior if and only if Δ is indefinite. In this case, Ξ can be defined by the set of $G(e^{j\omega}, t) \in \mathbb{C}$ such that

$$\begin{bmatrix} \Re(G(e^{j\omega}, t)) \\ \Im(G(e^{j\omega}, t)) \end{bmatrix} = U_\delta x - W_\delta^\dagger q \quad (6)$$

where is parametrised by a vector $x \in \mathbb{R}^2$ satisfying

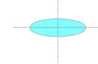

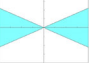
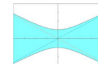
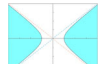
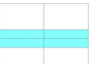
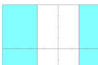

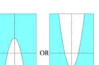
$$\begin{aligned} x^T \Lambda x + 2\alpha^T x + \beta &\leq 0 & \alpha &:= (\mathbf{I} - \Lambda \Lambda^\dagger) U_\delta^T q \\ & & \beta &:= r - q^T W_\delta^\dagger q. \end{aligned} \quad (7)$$

In particular, Ξ defines one of the nine regions in x -plane shown in Table 1 through a rotation by U_δ and a shift by $-W_\delta^\dagger q$. Moreover, with the help of STL syntax, STL can present complex zonotope in x -plane and the zonotope can evolve with time as shown in Figure 1.

Inspired by signal temporal logic (Donzé & Maler, 2010), STL can be equipped with quantitative semantics, called *robustness degree*, which quantifies how well a given set of matrices satisfies an STL formula, which is defined recursively as:

$$\begin{aligned} \rho(G(e^{j\omega}, t), \mu) &= \eta - \|G(e^{j\omega}, t)\|_\infty \\ \rho(G(e^{j\omega}, t), \mu') &= \|G(e^{j\omega}, t)\|_\infty - \eta \\ \rho(G(e^{j\omega}, t), \square_{[\omega_1, \omega_2]}\mu) &= \inf_{\omega' \in [\omega_1 + \omega, \omega_2 + \omega]} \rho(G(e^{j\omega'}, t), \mu) \\ \rho(G(e^{j\omega}, t), \diamond_{[\omega_1, \omega_2]}\mu') &= \sup_{\omega' \in [\omega_1 + \omega, \omega_2 + \omega]} \rho(G(e^{j\omega'}, t), \mu') \\ \rho(G(e^{j\omega}, t), \square_{[a, b]}\diamond_{[\omega_1, \omega_2]}\mu') &= \rho(G(e^{j\omega}, t'), \wedge_{a+t}^{b+t} \diamond_{[\omega_1 + v(t'), \omega_2 + v(t')]}\mu') \\ \rho(G(e^{j\omega}, t), \square_{[a, b]}\square_{[\omega_1, \omega_2]}\mu) &= \rho(G(e^{j\omega}, t'), \wedge_{a+t}^{b+t} \square_{[\omega_1 + v(t'), \omega_2 + v(t')]}\mu) \\ \rho(G(e^{j\omega}, t), \boxplus_{[a, b]}\diamond_{[\omega_1, \omega_2]}\mu') &= \rho(G(e^{j\omega}, t'), \vee_{a+t}^{b+t} \diamond_{[\omega_1 + v(t'), \omega_2 + v(t')]}\mu') \end{aligned}$$

Table 1. Nine cases of various regions (Iwasaki & Hara, 2005) and regions combinations.

Parameters	Values	Regions	Values	Regions	Values	Regions
α	0		0		0	
ζ_1	+		-		-	
ζ_2	+		-		+	
β	-		+		0	
α	0		0		0	
ζ_1	-		-		0	
ζ_1	+		+		0	
ζ_2	+		+		+	
β	-		+		-	
α	0		$\neq 0$		$\neq 0$	
ζ_1	-		0		-	
ζ_1	0		0		0	
ζ_2	0		0		0	
β	+		any		any	

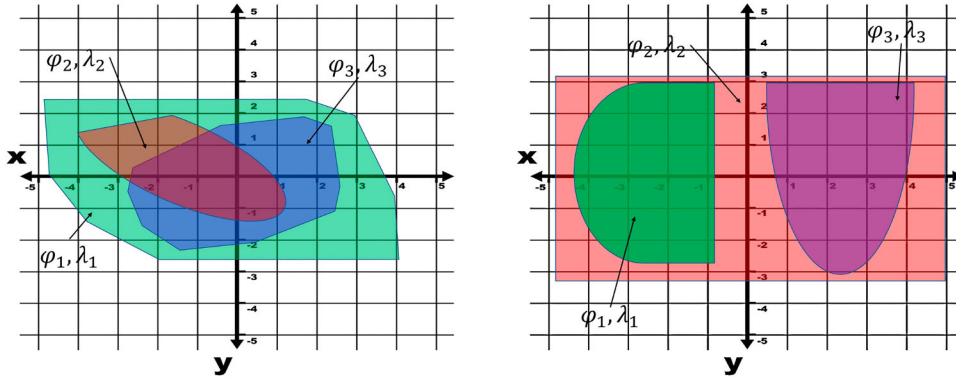


Figure 1. Regions combination with STL syntax leads to Zonotope.

$$\begin{aligned}
& \rho(G(e^{j\omega}, t), \boxplus_{[a,b]} \boxminus_{[\omega_1, \omega_2]} \mu) \\
&= \rho(G(e^{j\omega}, t'), \sqrt{a+t} \boxminus_{[\omega_1 + v(t'), \omega_2 + v(t')]} \mu) \\
& \rho(G(e^{j\omega}, t), \psi_1 \wedge \psi_2) \\
&= \min(\rho(G(e^{j\omega}, t), \psi_1), \rho(G(e^{j\omega}, t), \psi_2)) \\
& \rho(G(e^{j\omega}, t), \psi_1 \vee \psi_2) \\
&= \max(\rho(G(e^{j\omega}, t), \psi_1), \rho(G(e^{j\omega}, t), \psi_2)) \\
& \rho(G(e^{j\omega}, t), \varphi_1 \wedge \varphi_2) \\
&= \min(\rho(G(e^{j\omega}, t), \varphi_1), \rho(G(e^{j\omega}, t), \varphi_2)) \\
& \rho(G(e^{j\omega}, t), \varphi_1 \vee \varphi_2) \\
&= \max(\rho(G(e^{j\omega}, t), \varphi_1), \rho(G(e^{j\omega}, t), \varphi_2))
\end{aligned}$$

where $v(t)$ is a frequency shift caused by time t . For simplicity, and with a slight abuse of notation, here we will use $\rho(G, \varphi)$ to denote $\rho(G(e^{j\omega}, t), \varphi)$. Furthermore, if $\rho(G, \varphi)$ is large and positive, then G would have to deviate substantially to violate φ . In other words, $\rho(G, \varphi)$ characterises how robust $G(e^{j\omega}, t)$ is in the context of satisfying φ , while withstanding changes in $G(e^{j\omega}, t)$. For example, $G \models_t \boxminus_{[a,b]} \boxminus_{[\omega_1, \omega_2]} \mu$, if φ holds at every frequency between ω_1 and ω_2 for every time within $[a, b]$, i.e. $\rho(G(e^{j\omega}, t), \varphi) \geq 0$. When setting matrix $\Pi = \text{diag}\{\mathbf{I}, -\eta^2 \mathbf{I}\}$ and $\varphi = \boxminus_{[a,b]} \boxminus_{[\omega_1, \omega_2]} (f(G(e^{j\omega}, t), \Pi) < 0)$, if $\rho(G, \varphi)$ is large and positive, this indicates that $G(e^{j\omega}, t)$ is robust to noise with respect to φ within time interval $[a, b]$ (i.e. it is hard for noise to change the satisfaction status of $G(e^{j\omega}, t)$). A system defined by matrix $G(e^{j\omega}, t)$ satisfies φ at time t , denoted as $G \models_t \varphi$. The robustness is sound, i.e. $G \models_t \varphi \Leftrightarrow \rho(G(e^{j\omega}, t), \varphi) \geq 0$.

Definition 2.2 (Frequency range): In this paper, the frequency range Γ of a given parametric matrix $G(e^{j\omega}, t)$ with respect to Φ , $\Psi \in \mathbb{H}_2$ is defined as:

$$\Gamma(\Phi, \Psi) := \{s \in \mathbb{C} \mid f(s, \Phi) = 0, f(s, \Psi) \geq 0\}, \quad (8)$$

where f is defined by (3), and $\Phi, \Psi \in \mathbb{H}_2$ are given matrices that specify the geometry of Γ . In this paper, we have $\Gamma := \{\omega \mid \omega_1 \leq \omega \leq \omega_2\}$, defined by a centre frequency $\omega_c = (\omega_1 + \omega_2)/2$, radius $\omega_r = (\omega_2 - \omega_1)/2$ and

$$\Phi = \begin{bmatrix} -1 & 0 \\ 0 & 1 \end{bmatrix}, \quad \Psi = \begin{bmatrix} 0 & e^{j\omega_c} \\ e^{-j\omega_c} & -2 \cos \omega_r \end{bmatrix}. \quad (9)$$

2.1 Motivation example

Example 2.1: MEMS devices have gained tremendous attention due to their various applications, e.g. MEMS resonators (Ghayesh et al., 2013; Kim et al., 2008). The list of advantages includes low power consumption, low cost, and improved reliability. MEMS resonators are vibrating mechanical systems, in which the kinetic and potential energies are continuously exchanged. However, as electromechanical devices are scaled downward, introduction becomes increasingly difficult, hampering efforts to create finely controlled integrated systems.

One of the most straightforward MEMS actuation methods, based on the piezoelectric (PZT) effect, provides a means of directly converting an electric field into mechanical strain and actuating the resonators. To resonate, a mechanical system must possess the capacity to contain both kinetic and potential energies. Therefore, the basic resonator structure is a mass-spring system and the dynamics can be described as,

$$\begin{aligned}
x(t) &= \frac{T^2}{M_{\text{eff}}} F_{\text{in}}(t) + 2x(t-T) - x(t-2T) \\
&\quad - \frac{T\xi_{\text{eff}}}{M_{\text{eff}}} x(t-T) - \frac{T^2 K_{\text{eff}}}{M_{\text{eff}}} x(t) \quad (10)
\end{aligned}$$

where F_{in} is the input actuation force applied to the device, M_{eff} is the effective mass of the system, K_{eff} is the effective stiffness, T is the sampling period in the discrete-time system, and ξ_{eff} represents the effective damping coefficient. An example of the MEMS resonator schematic can be seen in Figure 2. Figure 2(a) shows a micrograph of electrostatically coupled two in-plane micro-cantilevers from Chappanda et al. (2018), which was fabricated from SI-on-insulator (SOI) wafers. Figure 2(b) shows the schematic of the device with its dimensions. It consists of two in-plane parallel cantilever beams that are slightly different in length along with two corresponding electrodes (F1 and F2). Figure 2(c) shows the first two resonant modes shapes of the coupled micro-cantilevers, where the cantilevers are actuated by the piezoelectric effect. The exciting signal will cause the vibration of the cantilever, which has two modes (in plane and out-of-plane) and the out-of-plane mode is used to realise the logic gates. The output voltage is measured at the fixed electrode F_1 and the resonant mode 1 is used to realise the logic gates. The mass-spring system model for the MEMS resonator can be seen in Figure 2(d), where the V_B is a shifting parametric voltage applied to electrodes B_2 in (10). Figure 2(e) shows

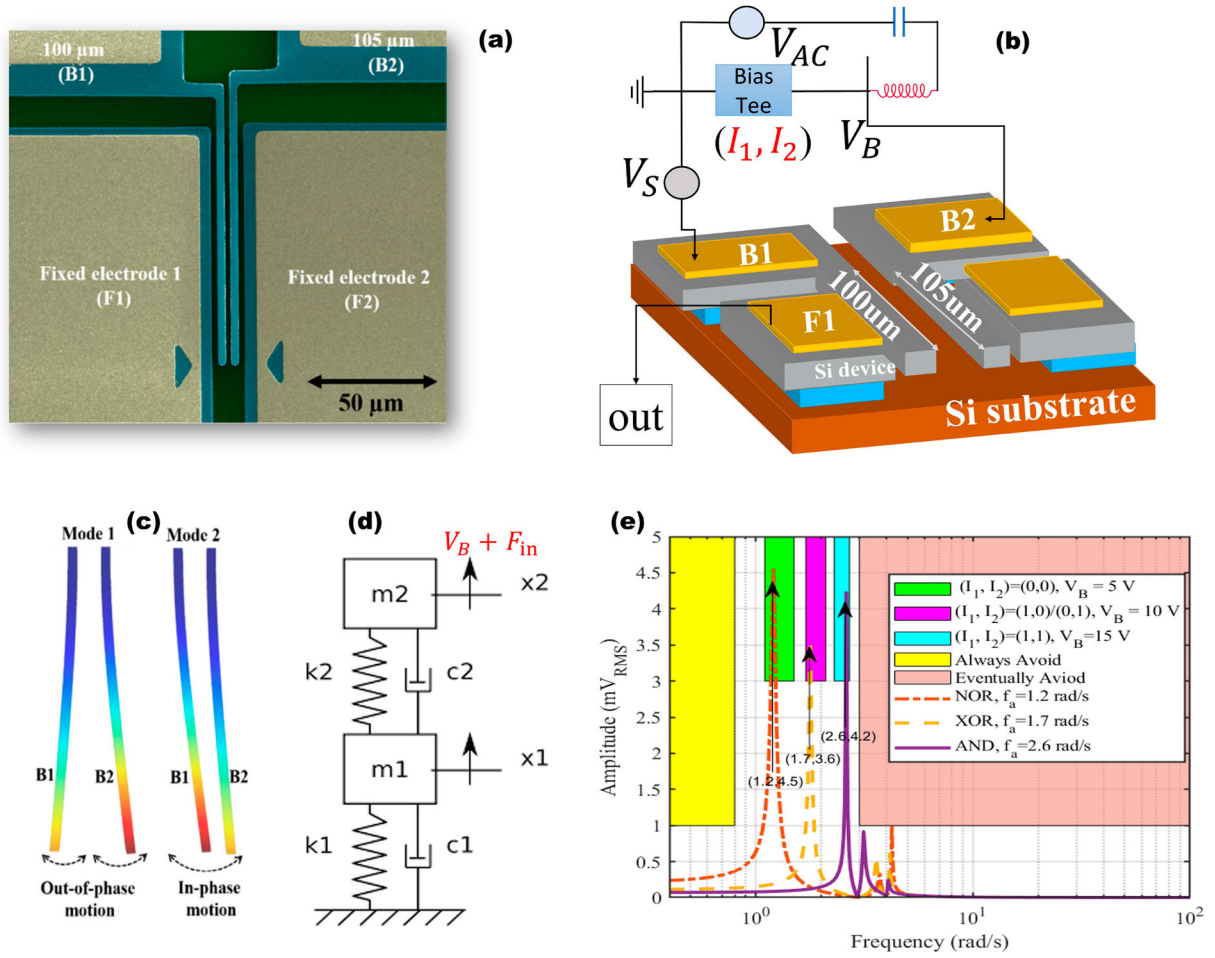


Figure 2. Device structure and schematics. (a) Micrograph of electrostatically coupled two in-plane micro-cantilevers from Chappanda et al. (2018). (b) A schematic showing the device with its dimensions. (c) The first two resonant modes shapes of the coupled micro-cantilevers. (d) The spring-mass model of the micro-cantilevers. (e) Frequency response of the coupled system at the different input voltage V_B encoded by (I_1, I_2) to realise different logic gates with different actuation frequency f_a .

the frequency response of the coupled system at different input voltages V_B at different time, in which we can see the input voltages, encoded by (I_1, I_2) with a bias tee, shift the resonant frequency.

When we want to use the MEMS device to realise the electro-mechanical logic gates, we hope the device has a higher shift in resonance frequency, which allows a decisive switch between the logic '1' and '0'. For example, Figure 2(e) shows three different resonance curves shift by $V_B = 5V$, $V_B = 10V$, and $V_B = 15V$, respectively, in which the increase of the input voltage V_B will move the resonance peaks to higher frequency regions. This mechanism can be used to realise 2-bit logic NOR, 2-bit XOR, and 2-bit AND with different activation frequencies, in which the value of V_B is controlled by 2-bit logic values (I_1, I_2) . For example, '1,0' or '0,1' will set V_B to 10 V with the bias tee, and the device will have resonance under a 1.7 rad/s exciting signal, leading to Boolean '1'. Likewise when the input is '0,0', or '1,1', leading to $V_B = 5V$ or $V_B = 15V$, no resonance is activated at 1.7 rad/s, and the output voltage is low, i.e. Boolean '0', which is a 2-bit XOR gate. Similarly, we can use the device to realise 2-bit AND gate, in which the activation frequency is set to 2.6 rad/s and a 2-bit NOR gate under activation frequency at 1.2 rad/s. In the other words, the MEMS device can

realise different logic operation by changing the exciting frequency. In order to have good performance in logic operations, the frequency shift caused by the bias voltage should be large. Therefore, when we design and control a MEMS device, the basic goal is to tune its frequency response pattern, i.e. the frequency response curve should satisfy some frequency domain specifications.

Assume we want the MEMS device to realise a cyclic sequence of logic operations by exciting the device with specific AC signals within time interval $[0, 3)$. For example, if we want the device to realise NOR, XOR, AND gate sequentially (as shown in Figure 2(e)), then the frequency temporal domain specifications, φ_{mems} , can be formally defined in STL as:

$$\begin{aligned} \varphi_{mems} &= \square_{[0,3)}(\varphi_1 \wedge \varphi_2 \wedge \varphi_3) \\ \varphi_1 &= \diamond_{[v(t), 0.1+v(t)]}(f(G(e^{j\omega}, t), \Pi_1) < 0) \\ \varphi_2 &= \square_{[1,4]}(f(G(e^{j\omega}, t), \Pi_2) < 0) \\ \varphi_3 &= \square_{[0.1, 0.2]}(f(G(e^{j\omega}, t), \Pi_2) < 0), \end{aligned} \quad (11)$$

where $G(e^{j\omega}, t)$ is the frequency response of the MEMS device at time t , $\Pi_1 = \text{diag}(-\mathbf{I}, 4\mathbf{I})$ requires the amplitude should be larger than 2, $\Pi_2 = \text{diag}(\mathbf{I}, -\mathbf{I})$ requires the amplitude should be smaller than 1; $\diamond_{[v(t), 0.4+v(t)]}$ indicates the frequency interval,

where $v(t) = 0.1t$, and φ_1 shows the device will be eventually activated to a high output with activation frequencies between $v(t)$ and $0.1 + v(t)$ rad/s; φ_2 and φ_3 shows the device will output low voltages when the activation frequencies are out of $[v(t), 0.4 + v(t)]$, $\square_{[0,3]}$ indicates the requirements should be satisfied at time 0, 1, and 2, respectively.

3. Problem formulation

Consider a n_s -order discrete-time LPV system \mathcal{S} with its state-space model as follows:

$$\begin{aligned} x^+(t) &= A(\vartheta(t))x(t) + B(\vartheta(t))w(t) + B_u(\vartheta(t))u(t) \\ z(t) &= C(\vartheta(t))x(t) + D(\vartheta(t))w(t) + D_u(\vartheta(t))u(t) \\ y(t) &= C_y(\vartheta(t))x(t) + D_y(\vartheta(t))w(t) \end{aligned} \quad (12)$$

where $x(t) \in \mathbb{R}^{n_s}$ is the state vector, $w(t) \in \mathbb{R}^{n_w}$, $u(t) \in \mathbb{R}^{n_u}$ are the external and control inputs, respectively, $y(t) \in \mathbb{R}^{n_y}$, $z(t) \in \mathbb{R}^{n_z}$ are the measured and controlled outputs, respectively. $x^+(t)$ represents $x(t+1)$. The dynamic of the system is parametrised by $\vartheta(t)$. To simplify the notation, we use ϑ to present $\vartheta(t)$ in the rest of this paper. Matrices

$$W(\vartheta) \triangleq (A(\vartheta), B(\vartheta), B_u(\vartheta), C(\vartheta), D(\vartheta), \\ D_u(\vartheta), C_y(\vartheta), D_y(\vartheta))$$

are real-valued, parameter-varying matrices, and are assumed to belong a polytopic parametric domain defined as

$$\mathbb{W} = \left\{ W(\theta) \mid W(\theta) = \sum_i^r \theta_i W_i(\vartheta); \theta \in \Delta \right\}, \quad (13)$$

where $W_i \triangleq (A_i, B_i, B_{u,i}, C_i, D_i, D_{u,i}, C_{y,i}, D_{y,i})$ are given matrices denote the basic system matrices, where $A_i \in \mathbb{R}^{n_s \times n_s}$, $B_i \in \mathbb{R}^{n_s \times n_w}$, $B_{u,i} \in \mathbb{R}^{n_s \times n_u}$, $C_i \in \mathbb{R}^{n_z \times n_s}$, $D_i \in \mathbb{R}^{n_z \times n_w}$, $D_{u,i} \in \mathbb{R}^{n_z \times n_u}$, $C_{y,i} \in \mathbb{R}^{n_y \times n_s}$, $D_{y,i} \in \mathbb{R}^{n_y \times n_w}$ denotes the system dynamics, and

$$\Delta \triangleq \left\{ \theta \in \mathbb{R}^r \mid \sum_i^r \theta_i = 1, \theta_i \geq 0, i = 1, \dots, r \right\}. \quad (14)$$

where r is the number of basic system matrices, and matrices W_i are constant (the parameter t is assumed to be known and fixed when ϑ is the unknown parameter) and matrix $W(\vartheta)$ is a linear combination of W_i , $i = 1, \dots, r$. In the rest of this paper, we use $A, B, B_u, C, D, D_u, C_y, D_y$ to denote $A(\vartheta), B(\vartheta), B_u(\vartheta), C(\vartheta), D(\vartheta), D_u(\vartheta), C_y(\vartheta), D_y(\vartheta)$ for short.

To stabilise the system \mathcal{S} , we are interested in finding a static output-feedback (SOF) controller

$$u(t) = K_s y(t), \quad (15)$$

where K_s is the SOF gain matrix and the closed-loop system $G_{cl,\vartheta,K_s}(s)$ can then be written as:

$$x(t)^+ = \mathbf{A}x(t) + \mathbf{B}w(t), \quad z(t) = \mathbf{C}x(t) + \mathbf{D}w(t), \quad (16)$$

with $G_{cl,\vartheta,K_s}(z) \triangleq \mathbf{C}(z\mathbf{I} - \mathbf{A})^{-1}\mathbf{B} + \mathbf{D}$, where

$$\begin{bmatrix} \mathbf{A} & \mathbf{B} \\ \mathbf{C} & \mathbf{D} \end{bmatrix} \triangleq \begin{bmatrix} A + B_u K_s C_y & B + B_u K_s D_y \\ C + D_u K_s C_y & D + D_u K_s D_y \end{bmatrix}. \quad (17)$$

Finally, the co-design problem to be addressed in this paper can be formulated as:

Problem 3.1: Given a spectral temporal logic formula φ defined by the syntax in (2), find a control gain K_s^* in (15) for system \mathcal{S} and a physical parameter vector $\theta^* \in \Delta$, such that the closed-loop system in (16) is asymptotically stable and satisfies STL formula φ .

The main input for the co-design problem is an STL formula φ (or a collection of them) that specifies spectral temporal domain requirements that the to-be-designed closed-loop system G_{cl,ϑ,K_s} must satisfy. The STL formula φ can be obtained from a human designer, and acts to constrain the optimisation problem. For example, if we set matrix Π such that it has the form $\text{diag}\{\mathbf{I}, -\eta^2 \mathbf{I}\}$, it leads to a bounded realness $\|G_{cl,\vartheta,K_s}\|_\infty < \eta$ for predicate formula μ or unbounded realness $\|G_{cl,\vartheta,K_s}\|_\infty \geq \eta$ for predicate formula μ' , where $\|G_{cl,\vartheta,K_s}\|_\infty$ can be understood as the H_∞ gain of G_{cl,ϑ,K_s} . The problem defined in Problem 3.1 is a co-design problem. Due to the min/max operators in the calculation of robustness, the constraints are not smooth and are non-differentiable. To address this problem, the results derived in Section 4 transform the above constraints into MILMIs with some assumptions, and solve the problem by SDPs.

4. Main results

In this section, we will show how to solve the Problem 3.1, which provides the theoretical foundation for transforming the STL formula specifications into a set of MILMIs.

4.1 The generalised STL lemma

When STL formulas are used to define frequency domain specifications for an LPV system with closed-loop system matrices $(\mathbf{A}, \mathbf{B}, \mathbf{C}, \mathbf{D})$, the formulas are endowed with a few nice properties. In particular, the following lemmas will show (i) how to combine simple STL specifications into more complicated ones and (ii) the relationship between STL specifications and the state-space realizations of LPV systems. In this section, we assume the parameter is fixed, thus the system can be seen as linear time-invariant (LTI) system and we use $G_{cl,\vartheta,K_s}(z)$ to denote $G_{cl,\vartheta,K_s}(z, t)$ in the rest of this section.

Lemma 4.1: *Let an STL formula $\varphi = \square_{[\omega_1, \omega_2]}(f(G_{cl,\vartheta,K_s}(z), \Pi) < 0)$, an LPV system $(\mathbf{A}, \mathbf{B}, \mathbf{C}, \mathbf{D})$ and its closed-loop transfer function $G_{cl,\vartheta,K_s}(z)$ be given. Then the following statements are equivalent:*

- (1) $\rho(G_{cl,\vartheta,K_s}(z), \varphi) > 0$ holds for $G_{cl,\vartheta,K_s}(z)$.
- (2) There exist matrices $P, Q \in \mathbb{H}_{n_s}$ such that $Q > 0$ and

$$M^*[\Phi_3 \otimes P + \Psi_3 \otimes Q]M + N^* \Pi N < 0, \quad (18)$$

where Ψ_3 and Φ_3 define the frequency range $[\omega_1, \omega_2]$, and can be obtained with (9), and

$$[M \mid N] \triangleq \begin{bmatrix} \mathbf{A} & \mathbf{B} & \mathbf{C} & \mathbf{D} \\ \mathbf{I} & 0 & 0 & \mathbf{I} \end{bmatrix}. \quad (19)$$

Proof: Based on the semantics of SL, formula $\square_{[\omega_1, \omega_2]}\varphi$ requires that the transfer function $G_{cl,\vartheta,K_s}(z)$ should satisfy the constraint defined by Π within range $[\omega_1 + \omega'_1, \omega_2 + \omega'_2]$,

which means $1 \Leftrightarrow 2$. Then the lemma can be proven based on the generalised KYP lemma in (Iwasaki & Hara, 2005). ■

Lemma 4.1 indicates that when STL formula is written as $\varphi = \square_{[\omega_1, \omega_2]}(f(G_{cl, \vartheta, K_s}(z), \Pi) < 0)$, which requires the frequency response is bounded by a value within frequency range $[\omega_1, \omega_2]$, the constraint defined by STL formula can be transformed into LMI (assume the parameter ϑ and K_s are fixed). This result is inline with traditional frequency domain specifications handled with the generalised KYP lemma in (1).

Lemma 4.2: Let STL formulas $\varphi_1 = \square_{[\omega_1, \omega_2]}(f(G_{cl, \vartheta, K_s}(z), \Pi_1) < 0)$, $\varphi_2 = \square_{[\omega'_1, \omega'_2]}(f(G_{cl, \vartheta, K_s}(z), \Pi_2) < 0)$, the state-space realisation of an LPV system $(\mathbf{A}, \mathbf{B}, \mathbf{C}, \mathbf{D})$ and its closed-loop transfer function $G_{cl, \vartheta, K_s}(z)$ be given. Moreover, frequency ranges $[\omega_1, \omega_2]$, $[\omega'_1, \omega'_2]$ are defined by matrices $\Phi, \Psi_1, \Psi_2 \in \mathbb{H}_2$. Then the following statements are equivalent:

- (1) $\rho(G_{cl, \vartheta, K_s}(z), \varphi_1 \vee \varphi_2) > 0$ holds for $G_{cl, \vartheta, K_s}(z)$.
- (2) There exist matrices $P, Q \in \mathbb{H}_{n_s}$, $Q > 0$, and a scalar $\tau > 0$ such that

$$M^*[\Phi \otimes P + \Psi \otimes Q]M + N^*\Pi N < 0, \quad (20)$$

where $\Psi = \Psi_1 + \Psi_2$ and $\Pi = \Pi_1 + \tau\Pi_2$.

Proof: 1) \Rightarrow 2). Based on the syntax of SL defined in Definition 2.1, and its semantics, formula φ_1 requires that the transfer function $G_{cl, \vartheta, K_s}(z)$ should satisfy the constraint defined by Π_1 within frequency range $[\omega_1, \omega_2]$ or the transfer function $G_{cl, \vartheta, K_s}(z)$ should satisfy the constraint defined by Π_2 within frequency range $[\omega'_1, \omega'_2]$. Based on the generalised KYP lemma in Iwasaki and Hara (2005), if there exist $P_1, P_2, Q_1, Q_2 \in \mathbb{H}_n$ and $Q_1, Q_2 > 0$, such that

$$M^*[\Phi \otimes P_1 + \Psi_1 \otimes Q_1]M + N^*\Pi_1 N < 0, \quad (21)$$

or

$$M^*[\Phi \otimes P_2 + \Psi_2 \otimes Q_2]M + N^*\Pi_2 N < 0, \quad (22)$$

then there exists $\tau > 0$, such that $(M^*[\Phi \otimes P_1 + \Psi_1 \otimes Q_1]M + N^*\Pi_1 N) + \tau(M^*[\Phi \otimes P_2 + \Psi_2 \otimes Q_2]M + N^*\Pi_2 N) < 0$ holds. Set P, Q , such that $P = P_1 + \tau P_2$, $\Psi \otimes Q = \Psi_1 \otimes Q_1 + \tau\Psi_2 \otimes Q_2$, $\Psi = \Psi_1 + \tau\Psi_2$ and $\Pi = \Pi_1 + \tau\Pi_2$, then (20) holds. Therefore, statement 2) holds.

2) \Rightarrow 1). We prove it by contradiction. If 1) does not hold, which means for all $P_1, P_2, Q_1, Q_2 \in \mathbb{H}_n$ and $Q_1, Q_2 > 0$, $M^*[\Phi \otimes P_1 + \Psi_1 \otimes Q_1]M + N^*\Pi_1 N \geq 0$, and $M^*[\Phi \otimes P_2 + \Psi_2 \otimes Q_2]M + N^*\Pi_2 N \geq 0$. Then for all $P, Q \in \mathbb{H}_n$, $\Psi = \Psi_1 + \Psi_2$ and $\Pi = \Pi_1 + \tau\Pi_2$, we have $M^*[\Phi \otimes P + \Psi \otimes Q]M + N^*\Pi N \geq 0$. It is easy to find 2) does not hold. Therefore, the lemma has been proven. ■

Lemma 4.2 addresses the formulas generated by syntax $\psi := \psi_1 \vee \psi_2$, where ψ_1 and ψ_2 have the form $\square_{[\omega_1, \omega_2]}\mu$. The LMI in (20) indicates that STL formulas generated with disjunction syntax can also be transformed into LMI constraints. Moreover, the basic formulas in this lemma are same with traditional frequency domain specifications, i.e. frequency response is bounded within a frequency range, but the combinations of

basic formulas are different from traditional ones. When the formula is generated by syntax $\varphi := \varphi_1 \wedge \varphi_2$, since the condition for the satisfaction of φ_1 and φ_2 can be presented as LMIs, then the condition for $\varphi := \varphi_1 \wedge \varphi_2$ is that all the LMIs for φ_1 and φ_2 are satisfied simultaneously. The disjunction operator is useful in many application domains, such as MEMS logic devices to represent the OR gate.

Lemma 4.3: Let an STL formula $\varphi = \diamond_{[\omega_1, \omega_2]}(f(G_{cl, \vartheta, K_s}(z), \Pi) < 0)$, an LPV system $(\mathbf{A}, \mathbf{B}, \mathbf{C}, \mathbf{D})$ and its closed-loop transfer function $G_{cl, \vartheta, K_s}(z)$ be given. Then the following statements are equivalent:

- (1) $\rho(G_{cl, \vartheta, K_s}(z), \varphi) > 0$ holds for $G_{cl, \vartheta, K_s}(z)$.
- (2) There exists a nonzero matrix $H \in \mathbb{H}_{n_s + n_w}$ and $H \geq 0$, such that

$$\begin{bmatrix} \mathbf{A} & \mathbf{B} & | & \mathbf{I} & \mathbf{0} \end{bmatrix} [\Phi \otimes H] \begin{bmatrix} \mathbf{A} & \mathbf{B} & | & \mathbf{I} & \mathbf{0} \end{bmatrix}^* = 0. \quad (23)$$

$$\begin{bmatrix} \mathbf{A} & \mathbf{B} & | & \mathbf{I} & \mathbf{0} \end{bmatrix} [\Psi^T \otimes H] \begin{bmatrix} \mathbf{A} & \mathbf{B} & | & \mathbf{I} & \mathbf{0} \end{bmatrix}^* \geq 0. \quad (24)$$

$$\text{tr}(\bar{\Pi}NHN^*) \geq 0. \quad (25)$$

where $\Pi = \text{diag}\{\mathbf{I}, -\eta^2\mathbf{I}\}$ and $\bar{\Pi} = \text{diag}\{-\mathbf{I}, \eta^2\mathbf{I}\}$, or $\Pi = \text{diag}\{-\mathbf{I}, \eta^2\mathbf{I}\}$ and $\bar{\Pi} = \text{diag}\{\mathbf{I}, -\eta^2\mathbf{I}\}$.

Proof: 1) \Rightarrow 2). Based on the semantics of SL, formula φ requires that the transfer function $G_{cl, \vartheta, K_s}(z)$ should satisfy the constraint defined by Π within frequency range $[\omega_1, \omega_2]$, which means the SL formula $\varphi' = \square_{[\omega_1, \omega_2]}(f(G_{cl, \vartheta, K_s}(z), \Pi) < 0)$ does not hold. Based on the generalised KYP lemma in (Iwasaki & Hara, 2005), formula φ' does not hold if and only if there exists $\varepsilon > 0$, such that

$$N^*\Pi N + M^*[\Phi \otimes P + \Psi \otimes Q]M \leq \varepsilon\mathbf{I} \quad (26)$$

has no solution (P, Q) satisfying $P = P^*$ and $Q = Q^* \geq 0$. It then follows from the separating hyper plane argument (Lemma 11 in Iwasaki & Hara, 2005) that there exists a nonzero Hermitian matrix $H \geq 0$ such that

$$\text{tr}(H[N^*\Pi N + M^*[\Phi \otimes P + \Psi \otimes Q]M]) \geq 0 \quad (27)$$

holds for all $P = P^*$ and $Q = Q^* \geq 0$. Noting that this inequality is equivalent to

$$\begin{aligned} & \text{tr}([\Phi \otimes P]MHM^*) \\ & + \text{tr}([\Psi \otimes Q]MHM^*) + \text{tr}(\Pi(NHN^*)) \geq 0, \end{aligned}$$

holds for all $P = P^*$ and $Q = Q^* \geq 0$. Since we have

$$\begin{aligned} \text{tr}([\Phi \otimes P]MHM^*) &= \text{tr}(P[\mathbf{A} \ \mathbf{B}| \mathbf{I} \ \mathbf{0}][\Phi^T \otimes H][\mathbf{A} \ \mathbf{B}| \mathbf{I} \ \mathbf{0}]^*) \\ \text{tr}([\Psi \otimes Q]MHM^*) &= \text{tr}(Q[\mathbf{A} \ \mathbf{B}| \mathbf{I} \ \mathbf{0}][\Psi^T \otimes H][\mathbf{A} \ \mathbf{B}| \mathbf{I} \ \mathbf{0}]^*) \end{aligned} \quad (28)$$

Then the conditions are equivalent to there exists a nonzero Hermitian $H \geq 0$, such that,

$$\begin{bmatrix} \mathbf{A} & \mathbf{B} & | & \mathbf{I} & \mathbf{0} \end{bmatrix} [\Phi^T \otimes H] \begin{bmatrix} \mathbf{A} & \mathbf{B} & | & \mathbf{I} & \mathbf{0} \end{bmatrix}^* = 0. \quad (29)$$

$$\begin{bmatrix} \mathbf{A} & \mathbf{B} & \mathbf{I} & \mathbf{0} \end{bmatrix} [\Psi^T \otimes H] \begin{bmatrix} \mathbf{A} & \mathbf{B} & \mathbf{I} & \mathbf{0} \end{bmatrix}^* \geq 0. \quad (30)$$

$$\text{tr}(\Pi \mathbf{N} \mathbf{H} \mathbf{N}^*) \geq 0. \quad (31)$$

which are the same to the conditions defined in (23)–(25).

2) \Rightarrow 1). Statement 2) is equivalent to formula φ' does not hold. Based on the semantics of STL, statement 1) holds. The proof is completed. ■

Compared with traditional frequency domain specifications, the STL formula φ in Lemma 4.3 requires the amplitude of the frequency response has lower bound, but no upper bound is given. This property is useful in many applications, such as resonance and frequency activation devices, where the frequency response must be large in some frequency bands. However, the conditions in Lemma 4.3 are complex, to simplify the conditions, we have a conservative condition as follows.

Lemma 4.4: Let an STL formula $\varphi = \diamond_{[\omega_1, \omega_2]}(f(G_{cl, \vartheta, K_s}(z), \Pi) < 0)$, an LPV system $(\mathbf{A}, \mathbf{B}, \mathbf{C}, \mathbf{D})$ and its closed-loop transfer function $G_{cl, \vartheta, K_s}(z)$ be given. Then $\rho(G_{cl, \vartheta, K_s}(z), \varphi) > 0$ holds for $G_{cl, \vartheta, K_s}(z)$ if there exists $\omega' \in \mathbb{R}$ and $\omega' > \omega_c$, matrices $P, Q \in \mathbb{H}_{n_s}$ and $Q > 0$, such that

$$M^*[\Phi \otimes P + \Psi' \otimes Q]M + N^* \Pi N < 0, \quad (32)$$

where Ψ' defines the frequency range $[\omega_c, \omega']$.

Proof: (Sketch) The formula φ denotes that $f(G_{cl, \vartheta, K_s}(z), \Pi) < 0$ is satisfied at least once within frequency range $[\omega_1, \omega_2]$, while the condition in (32) indicates that $f(G_{cl, \vartheta, K_s}(z), \Pi) < 0$ is always satisfied within frequency range $[\omega_c, \omega']$, thus the proof is complete. ■

Lemma 4.5: Let STL formulas $\varphi_1 = \square_{[\omega'_1, \omega'_2]}(f(G_{cl, \vartheta, K_s}(z), \Pi) < 0)$, $\varphi_2 = \diamond_{[\omega_1, \omega_2]}(f(G_{cl, \vartheta, K_s}(z), \Pi') < 0)$, $\varphi = \varphi_1 \wedge \varphi_2$, an LTI system $(\mathbf{A}, \mathbf{B}, \mathbf{C}, \mathbf{D})$ and its closed-loop transfer function $G_{cl, \vartheta, K_s}(z)$ be given. Then the following statements are equivalent:

- (1) $\rho(G_{cl, \vartheta, K_s}(z), \varphi) > 0$ holds for $G_{cl, \vartheta, K_s}(z)$.
- (2) There exist matrices $P, Q \in \mathbb{H}_{n_s}$ and a nonzero matrix $H \in \mathbb{H}_{n_s + n_w}$, such that $H, Q \geq 0$, and

$$M^*[\Phi \otimes P + \Psi \otimes Q]M + N^* \Pi N < 0, \quad (33a)$$

$$\text{tr}(\bar{\Pi}' \mathbf{N} \mathbf{H} \mathbf{N}^*) \geq 0, \quad (33b)$$

$$\begin{bmatrix} \mathbf{A} & \mathbf{B} & \mathbf{I} & \mathbf{0} \end{bmatrix} [\Phi \otimes H] \begin{bmatrix} \mathbf{A} & \mathbf{B} & \mathbf{I} & \mathbf{0} \end{bmatrix}^* = 0, \quad (33c)$$

$$\begin{bmatrix} \mathbf{A} & \mathbf{B} & \mathbf{I} & \mathbf{0} \end{bmatrix} [\Psi \otimes H] \begin{bmatrix} \mathbf{A} & \mathbf{B} & \mathbf{I} & \mathbf{0} \end{bmatrix}^* \geq 0. \quad (33d)$$

Proof: Based on Lemmas 4.1 and 4.3, the theorem can be easily proven. Here we omit the detail. ■

Remark 4.1: Lemma 4.1 gives the satisfaction conditions for $\square_{[\omega_1, \omega_2]} \psi$. Lemma 4.2 is for $\varphi_1 \wedge \varphi_2$ and $\psi_1 \vee \psi_2$. Lemma 4.3 is for $\diamond_{[\omega_1, \omega_2]} \mu$. Lemma 4.4 relaxes the constraints in Lemma 4.3, which transfers the sufficient and necessity conditions into sufficient conditions. Note that ω' can be set as $\omega_c + \iota$ to simply

the conditions, where ι is a sufficient small positive real number. Lemma 4.5 is for $\diamond_{[\omega_1, \omega_2]} \mu \wedge \square_{[\omega'_1, \omega'_2]} \mu$. Thus, Lemmas 4.1–4.5 cover all the syntax of SL defined in (2). Based on these results, we can get a generalised STL lemma as follows.

Theorem 4.1 (Generalized STL lemma): Let an STL formula φ , an LPV system $(\mathbf{A}, \mathbf{B}, \mathbf{C}, \mathbf{D})$ and its closed-loop transfer function at time t , $G_{cl, \vartheta, K_s}(z)$ be given. Then the following statements are equivalent:

- (1) $\rho(G_{cl, \vartheta, K_s}(z), \varphi) > 0$ holds for $G_{cl, \vartheta, K_s}(z)$.
- (2) There exist nonzero matrices $H_j \in \mathbb{H}_{n_s + n_w}$, matrices $P_i, Q_i \in \mathbb{H}_{n_s}$ and $H_j, Q_i \geq 0$, $i = 1, 2, \dots, I, j = 1, 2, \dots, J$, such that

$$M^*[\Phi \otimes P_i + \Psi_i \otimes Q_i]M + N^* \Pi_i N < 0, \quad (34a)$$

$$\text{tr}(\Pi_j \mathbf{N} \mathbf{H}_j \mathbf{N}^*) \geq 0, \quad (34b)$$

$$\hat{M}^T [\Phi \otimes H_j] \hat{M} = 0, \quad (34c)$$

$$\hat{M}^T [\Psi^T \otimes H_j] \hat{M} \geq 0. \quad (34d)$$

where $\hat{M} = \begin{bmatrix} \mathbf{A} & \mathbf{B} & \mathbf{I} & \mathbf{0} \end{bmatrix}^T$, Ψ_i, Π_i and Π_j are related to the formula φ , which is defined based on the atomic formula in Lemmas 4.1–4.4.

Proof: Lemma 4.1 to 4.5 can be extended to any STL formula. All the other formulas' satisfaction conditions can be derived based on these Lemmas. Therefore, the theorem can be derived accordingly. ■

4.2 Co-design decoupling

Section 4.1 transforms the STL formula constraints at time t into LMIs with a given vector ϑ . When parameter vector ϑ is free to be selected, the constraints are neither LMIs nor BMIs. This section introduces how to decouple the product term between control parameters and physical parameters.

Theorem 4.2: Let an STL formula φ as defined in Theorem 4.1, $K_s \in \mathbb{R}^{n_u \times n_y}$, physical parameter $\theta \in \mathbb{R}^r$, and an LPV system in (12) be given. The closed-loop system $G_{cl, \vartheta, K_s}(e^{j\omega})$ is asymptotically stable and satisfies φ , if and only if there exist matrices $P_i, Q_i \in \mathbb{H}_{n_s}$, $P_{si} \in \mathbb{S}_{n_s}$ and $F \in \mathbb{R}^{n_u \times n_u}$, $E_1 \in \mathbb{R}^{n_s \times n_u}$, $E_2 \in \mathbb{R}^{n_w \times n_u}$, $E_3 \in \mathbb{R}^{n_y \times n_s}$, $Z \in \mathbb{R}^{n_s \times n_s}$, $H_j \in \mathbb{H}_{n_s + n_w}$, such that $P_{si} > 0, Q_i > 0, H_j \geq 0$ and

$$N_f^T \hat{\Xi}_i N_f + \Theta_i + \Theta_i^T < 0, \quad (35a)$$

$$N_s^T \hat{\Xi}_s N_s + \Theta_s + \Theta_s^T < 0, \quad (35b)$$

$$M_f \hat{\Xi}_h M_f^T = 0, \quad (35c)$$

$$M_f \hat{\Xi}_j M_f^T + \Theta_j + \Theta_j^T \geq 0, \quad (35d)$$

$$\text{tr}(\Pi_j' \mathbf{N} \mathbf{H}_j \mathbf{N}^*) \geq 0, \quad (35e)$$

where $\hat{\Xi}_i = \text{diag}(\Phi \otimes P_i + \Psi_i \otimes Q_i, \Pi)$, $\hat{\Xi}_s = \Phi \otimes P_s$, $\hat{\Xi}_j = \Psi_j^T \otimes H_j$, $\hat{\Xi}_h = \Phi \otimes H_j$ and

$$\Theta_i \triangleq [E_1^T \ E_2^T \ -F^T]^T [K_s C_y \ K_s D_y \ -\mathbf{I}],$$

$$\begin{aligned}\Theta_s &\triangleq [E_1^T \quad -F_1^T]^T [K_s C_y \quad -\mathbf{I}], \\ \Theta_j &\triangleq [E_3^T \quad Z^T]^T [B_u K_s \quad -\mathbf{I}], \\ M_f &\triangleq \begin{bmatrix} A & B & \mathbf{I} & 0 \\ C_y & D_y & 0 & 0 \end{bmatrix}, \\ N_f &\triangleq \begin{bmatrix} A^T & \mathbf{I} & C^T & 0 \\ B^T & 0 & D^T & \mathbf{I} \\ B_u^T & 0 & D_u^T & 0 \end{bmatrix}^T, \quad N_s \triangleq \begin{bmatrix} A & B_u \\ \mathbf{I} & 0 \end{bmatrix},\end{aligned}$$

Proof: *Sufficiency:* The LMI in (1) can be re-written into the following form

$$\hat{W}^T \hat{\Xi}_i \hat{W} < 0 \quad (36)$$

where

$$\hat{W} \triangleq \begin{bmatrix} \mathbf{A}^T & \mathbf{I} & \mathbf{C}^T & 0 \\ \mathbf{B}^T & 0 & \mathbf{D}^T & \mathbf{I} \end{bmatrix}^T \quad (37)$$

To guarantee the stability of the system, the following Lyapunov inequality should hold:

$$\hat{W}_s^T \hat{\Xi}_s \hat{W}_s < 0; \quad \hat{W}_s = [\mathbf{A}^T \quad \mathbf{I}]^T. \quad (38)$$

Suppose the conditions in (2) are satisfied for some $P_{si}, Q_i, H_j, E_1, E_2, F$. Note that

$$\begin{aligned}N_f T_1 &\equiv \hat{W}, [K_s C_y \quad K_s D_y \quad -\mathbf{I}] T_1 \equiv 0 \\ N_s T_{1s} &\equiv \hat{W}_s, [K_s C_y \quad -\mathbf{I}] T_1 \equiv 0 \\ T_{1e} M_f &\equiv \hat{M}, [B_{u,t} K_s, -\mathbf{I}] T_{1e}^T \equiv 0\end{aligned} \quad (39)$$

where

$$\begin{aligned}T_1 &\triangleq \begin{bmatrix} \mathbf{I} & 0 \\ 0 & I \\ K_s C_y & K_s D_y \end{bmatrix}, \quad T_{1e} \triangleq [\mathbf{I} \quad B_{u,t} K_s], \\ T_{1s} &\triangleq \begin{bmatrix} \mathbf{I} \\ K_s C_y \end{bmatrix},\end{aligned} \quad (40)$$

Multiplying the left- and right-hand sides of the conditions in (35a) by T_1^T and T_1 , respectively, we can obtain 36. Similarly, applying T_{1s} to condition (35b), T_{1e} to condition (35c) and condition (35d). Since we have (38) and the conditions in (34). Then using the Generalized SL lemma and Lyapunov inequality can complete the sufficient part.

Necessity: Suppose the system $G_{cl,\vartheta,K_s}(z)$ in (12) is asymptotically stable and satisfies the SL formula ϕ . Then the inequalities in (36),(38) and (34) hold for some $P_i, Q_i > 0, H_j > 0, P_s > 0$. Hence for some sufficiently large $\epsilon > 0$, the following dilated inequalities hold

$$\begin{aligned}\Xi_i &\triangleq \begin{bmatrix} \hat{W}^T \hat{\Xi}_i \hat{W} & \hat{W}^T \hat{\Xi}_i \hat{V} \\ \hat{V}^T \hat{\Xi}_i \hat{W} & \hat{V}^T \hat{\Xi}_i \hat{V} - \epsilon \mathbf{I} \end{bmatrix} < 0 \\ \Xi_s &\triangleq \begin{bmatrix} \hat{W}_s^T \hat{\Xi}_s \hat{W}_s & \hat{W}_s^T \hat{\Xi}_s \hat{V}_s \\ \hat{V}_s^T \hat{\Xi}_s \hat{W}_s & \hat{V}_s^T \hat{\Xi}_s \hat{V}_s - \epsilon \mathbf{I} \end{bmatrix} < 0 \\ \Xi_j &\triangleq \begin{bmatrix} \hat{W}_f^T \hat{\Xi}_j \hat{W}_f & \hat{W}_f^T \hat{\Xi}_j \hat{V}_f^T \\ \hat{V}_f^T \hat{\Xi}_j \hat{W}_f & \hat{V}_f^T \hat{\Xi}_j \hat{V}_f^T + \epsilon \mathbf{I} \end{bmatrix} \geq 0 \\ \Xi_h &\triangleq \begin{bmatrix} \hat{W}_f^T \hat{\Xi}_h \hat{W}_f & \hat{W}_f^T \hat{\Xi}_h \hat{V}_f^T \\ \hat{V}_f^T \hat{\Xi}_h \hat{W}_f & \hat{V}_f^T \hat{\Xi}_h \hat{V}_f^T \end{bmatrix} = 0\end{aligned} \quad (41)$$

where $\hat{V} \triangleq [B_u^T \quad 0 | D_u^T \quad 0]^T$, $\hat{V}_s \triangleq [B_u^T \quad 0]^T$, and $\hat{V}_f \triangleq [C_y \quad D_y \quad 0 \quad 0]$. Define

$$\begin{aligned}T &\triangleq \begin{bmatrix} \mathbf{I} & 0 & 0 \\ 0 & \mathbf{I} & 0 \\ -K_s C_y & -K_s D_y & \mathbf{I} \end{bmatrix}, \\ T_s &\triangleq \begin{bmatrix} \mathbf{I} & 0 \\ -K_s C_y & \mathbf{I} \end{bmatrix}, \quad T_j \triangleq \begin{bmatrix} \mathbf{I} & -B_u K_s \\ 0 & \mathbf{I} \end{bmatrix}\end{aligned} \quad (42)$$

Then inequalities in (41) imply

$$\begin{aligned}T^T \Xi_i T &= N_f^T \hat{\Xi}_i N_f + [-\epsilon K_s C_y \quad -\epsilon K_s D_y \quad \epsilon \mathbf{I}]^T \\ &\quad \times [K_s C_y \quad K_s D_y \quad -\mathbf{I}] < 0 \\ T_s^T \Xi_s T_s &= N_s^T \hat{\Xi}_s N_s + [-\epsilon K_s C_y \quad \epsilon \mathbf{I}]^T \times [K_s C_y \quad -\mathbf{I}] < 0 \\ T_j \Xi_j T_j^T &= M_f \hat{\Xi}_j M_f^T + [\epsilon B_u K_s \quad -\epsilon \mathbf{I}]^T \times [B_u K_s \quad -\mathbf{I}] \geq 0 \\ T_j \Xi_h T_j^T &= M_f \hat{\Xi}_h M_f^T = 0\end{aligned} \quad (43)$$

which changes to those in (43) by considering $F = -\frac{\epsilon}{2} \mathbf{I}$, $E_1 = -\frac{\epsilon}{2} (K_s C_y)^T$, $E_2 = -\frac{\epsilon}{2} (K_s D_y)^T$, $E_3 = \frac{\epsilon}{2} (B_u K_s)^T$, $Z = -\frac{\epsilon}{2} \mathbf{I}$. Then based on the conditions in (34), conditions (35c) and (35d) hold. The proof is completed. \blacksquare

Corollary 4.1: *Let an STL formula ϕ as defined in Theorem 4.1, parameter $\theta \in \mathbb{R}^r$, and an LPV system in (12) be given. An SOF controller in (15) exists such that the closed-loop system $G_{cl,\theta,K_s}(z)$ is asymptotically stable and satisfies ϕ , if and only if there exist matrices $P_i, Q_i \in \mathbb{H}_{n_s}$, $P_s \in \mathbb{S}_{n_s}$ and $F \in \mathbb{R}^{n_u \times n_u}$, $L \in \mathbb{R}^{n_u \times n_y}$, $K_1 \in \mathbb{R}^{n_u \times n_s}$, $K_2 \in \mathbb{R}^{n_u \times n_w}$, $E_3 \in \mathbb{R}^{n_y \times n_s}$, $Z \in \mathbb{R}^{n_s \times n_s}$, $H_j \in \mathbb{H}_{n_s+n_w}$, such that $P_s > 0, Q_i > 0, H_j \geq 0$ and*

$$N_f^T \hat{\Xi}_i N_f + \Upsilon_i + \Upsilon_i^T < 0, \quad (44a)$$

$$N_s^T \hat{\Xi}_s N_s + \Upsilon_s + \Upsilon_s^T < 0, \quad (44b)$$

$$M_f \hat{\Xi}_h M_f^T = 0, \quad (44c)$$

$$M_f \hat{\Xi}_j M_f^T + \Upsilon_j + \Upsilon_j^T \geq 0, \quad (44d)$$

$$\text{tr}(\Pi_j' N H_j N^*) \geq 0, \quad (44e)$$

where $\Upsilon \triangleq [K_1 \quad K_2 \quad -\mathbf{I}]^T [L C_y \quad L D_y \quad -F]$, $\Upsilon_s \triangleq [K_1 \quad -\mathbf{I}]^T [L C_y \quad -F]$, and $\Upsilon_j \triangleq \vartheta_j$. Moreover, if the above conditions are satisfied, the SOF controller gain in (15) is given by $K_s = F^{-1} L$.

Proof: Note that the second condition in (35b) implies that $F + F^T < 0$, thus F is invertible. Make change of variables $L = F K_s$, $K_1 = (E_1 F^{-1})^T$ and $K_2 = (E_2 F^{-1})^T$ for the conditions in (2). It is easy to find that if the conditions in (2) are satisfied, those in (44) are also satisfied with variables $L = F K_s$, $K_1 = (E_1 F^{-1})^T$ and $K_2 = (E_2 F^{-1})^T$. Conversely, since the second term in (44) also implies $F + F^T < 0$, if the conditions in (44) are satisfied, then those in (2) are also satisfied with $K_s = F^{-1} L$, $E_1 = K_1^T F$ and $E_2 = K_2^T F$. The proof is completed. \blacksquare

When the design parameter vector ϑ , and matrices K_1, K_2 are known, the conditions in (44) are linear constraints. However, when ϑ is free to select, there exist product terms in (44), which

leads to non-BMI constraints. The following theorem addresses this issue and transforms the conditions in (44) into a linear form.

Theorem 4.3: *Let an STL formula φ as defined in (2), parameter $\vartheta \in \mathbb{R}^r$, and an LPV system in (12) be given. The closed-loop system $G_{cl,\theta,K_s}(z)$ is asymptotically stable and satisfies φ , if there exist matrices $P_i, Q_i \in \mathbb{H}_{n_s}$, $P_s \in \mathbb{S}_{n_s}$ and real matrices U_i, V_s, R, K_1, K_2 , such that $P_s, Q_i > 0$ and*

$$\bar{\Xi}_i + X_i \Sigma_t + \Sigma_t^T X_i^T < 0, \quad (45a)$$

$$\bar{\Xi}_s + X_s \Sigma_{s,t} + \Sigma_{s,t}^T X_s^T < 0, \quad (45b)$$

where

$$\begin{aligned} \bar{\Xi}_i &\triangleq \begin{bmatrix} \hat{\Xi}_i & 0 \\ 0 & 0 \end{bmatrix}, \quad \bar{\Xi}_s \triangleq \begin{bmatrix} \hat{\Xi}_s & 0 \\ 0 & 0 \end{bmatrix}, \\ \Sigma_t &\triangleq \left[\begin{array}{cc|cc|c} -\mathbf{I} & A + B_u K_1 & 0 & B + B_u K_2 & B_u \\ 0 & C + D_u K_1 & -\mathbf{I} & D + D_u K_2 & D_u \\ 0 & K_s C_y - K_1 & 0 & K_s D_y - K_2 & -\mathbf{I} \end{array} \right], \\ \Sigma_{s,t} &\triangleq \left[\begin{array}{cc|c} -\mathbf{I} & A + B_u K_1 & B_u \\ 0 & K_s C_y - K_1 & -\mathbf{I} \end{array} \right], \\ X_i &\triangleq \begin{bmatrix} U_i & 0 \\ 0 & R \end{bmatrix}, \quad X_s \triangleq \begin{bmatrix} V_s & 0 \\ 0 & R \end{bmatrix}, \end{aligned}$$

Proof: Given two bounded matrices $K_1 \in \mathbb{R}^{n_u \times n_s}$ and $K_2 \in \mathbb{R}^{n_u \times n_w}$, based on Lemma 4.1–4.4, and then (36), (38) are equivalent to the following dilated matrix inequality conditions, respectively:

$$\begin{aligned} &\left[\begin{array}{cc} \hat{W} & \\ K_s C_y - K_1 & K_s D_y - K_2 \end{array} \right]^T \\ &\quad \times \bar{\Xi}_i \left[\begin{array}{cc} \hat{W} & \\ K_s C_y - K_1 & K_s D_y - K_2 \end{array} \right] < 0 \\ &\left[\begin{array}{c} \hat{W}_s \\ K_s C_y - K_1 \end{array} \right]^T \bar{\Xi}_i \left[\begin{array}{c} \hat{W}_s \\ K_s C_y - K_1 \end{array} \right] < 0 \end{aligned} \quad (46)$$

It can be verified that the null spaces of Σ and Σ_s can be chosen, respectively, as

$$\begin{aligned} \Sigma^\perp &= \left[\hat{W}^T [K_s C_y - K_1 \quad K_s D_y - K_2]^T \right]^T \\ \Sigma_s^\perp &= \left[\hat{W}_s^T [K_s C_y - K_1]^T \right]^T \end{aligned} \quad (47)$$

Then we can multiply the condition in (45) by $\Sigma^{\perp T}$ on the left and Σ^\perp on the right, and the condition in (45b) by $\Sigma_s^{\perp T}$ on the left and Σ_s^\perp on the right, respectively. Then,

$$\begin{aligned} \Sigma^{\perp T} (\bar{\Xi}_i + X_i \Sigma + \Sigma^T X_i^T) \Sigma^\perp < 0 &\Rightarrow \Sigma^{\perp T} \bar{\Xi}_i \Sigma^\perp < 0, \\ \Sigma_s^{\perp T} (\bar{\Xi}_s + X_s \Sigma_s + \Sigma_s^T X_s^T) \Sigma_s^\perp < 0 &\Rightarrow \Sigma_s^{\perp T} \bar{\Xi}_s \Sigma_s^\perp < 0, \end{aligned} \quad (48)$$

Accordingly, the right hand sides of ‘ \Rightarrow ’ in (48) are equivalent as the conditions in (46). Consequently, according to the generalised STL lemma and the Lyapunov inequality, the closed-loop system $G_{cl,\theta,K_s}(z)$ is guaranteed to be asymptotically stable and satisfy the STL formula φ . The theorem has been proven. \blacksquare

Remark 4.2: Theorem 4.1 shows sufficient and necessary conditions for a system to satisfy an STL formula φ at time t . However, the constraints in Equation (34) are non-linear (not BMIs or LMIs), which is impossible to check efficiently. Theorem 4.3 provides a way to check the conditions under the assumption that the physical parameter θ is given. When the physical parameter θ is given and fixed, the dynamic matrices, e.g. A, B_u , are fixed, and the satisfaction of the frequency domain specifications can be transformed into LMI or linear equation constraints. Namely, constraints depicted by Equation (45) are LMIs or linear equations. When the θ is the variable that needs to be optimised, the constraints are BMI and linear equations. But if we assume $\kappa = [K_1, K_2, K_s], \Upsilon = [U_i, V_s, R]$ are known in Theorem 4.3, which are matrices related to the controller, the constraints depicted by Equation (45) are LMIs or linear equations. In the other words, if we alternately optimise physical parameters and control parameters, the constraints are depicted by Equation (45) are LMIs or linear equations. Note that the theorems developed in this section is valid for all matrix $\Phi \in \mathbb{H}_{n+m}$, not only the Φ in STL semantic definition. Next, we will show how to solve the co-design problem when the temporal operators are applied in STL formula.

4.3 Quantitative encoding for spectral temporal logic

The robustness satisfaction of the STL specification provides a natural objective for the codesign problem. In this subsection, we sketch the mixed integer linear programming (MILP) encoding of the spectral formula and Boolean operators using the quantitative semantic and the encoding of the temporal operators, which follows the encoding method in Raman et al. (2014). Given a formula φ , we introduce a variable r_t^φ , and an associated set of MILP constraints such that $r_t^\varphi > 0$ if and only if φ holds at time t . When the MILP constraints generated recursively, such that r_0^φ determines whether a formula φ holds in the initial state. Moreover, we also enforce $r_t^\varphi = \rho(G_{cl,\vartheta,K_s}(e^{j\omega}, t), \varphi)$.

For each spectral formula $\psi \in S$, we now introduce variables r_t^ψ for time indices $t = 0, 1, \dots, N$. Then the Boolean operations are defined as:

$$\text{Conjunction: } \phi = \bigwedge_i^m \varphi_i$$

$$\sum_{i=1}^m p_{t_i}^{\varphi_i} = 1 \quad (49a)$$

$$r_t^\phi \leq r_{t_i}^{\varphi_i}, i = 1, \dots, m \quad (49b)$$

$$r_{t_i}^{\varphi_i} - (1 - p_{t_i}^{\varphi_i})M \leq r_t^\phi \leq r_{t_i}^{\varphi_i} + M(1 - p_{t_i}^{\varphi_i}) \quad (49c)$$

where $p_{t_i}^{\varphi_i}$ is a new binary variables for $i = 1, \dots, m$, and M is a sufficiently large positive number. Then Equation (49a) enforces that there is one and only one $j \in \{1, \dots, m\}$ such that $p_{t_j}^{\varphi_j} = 1$, Equation (49b) enforces that r_t^ϕ is smaller than all $r_{t_i}^{\varphi_i}$, and Equation (49c) ensures that $r_t^\phi = r_{t_j}^{\varphi_j} \iff p_{t_j}^{\varphi_j} = 1$. Together, these constraints enforce that $r_t^\phi = \min(r_{t_i}^{\varphi_i})$.

Disjunction: $\phi = \bigvee_i^m \varphi_i$ is encoded similarly to conjunction, replacing (49b) with $r_t^\phi \geq r_{t_i}^{\varphi_i}, i = 1, \dots, m$, which leads to $r_t^\phi = \max(r_{t_i}^{\varphi_i})$.

$$\text{Always: } \phi = \square_{[a,b]} \varphi$$

Let $a_t^N = \min(t+1, N)$ and $b_t^N = \min(t+b, N)$, where N is the bounded time for the formula. Then define $\phi' = \bigwedge_{a_t^N} \phi_i$, we have $r_t^\phi = r_t^{\phi'}$ and the encoding for the always operator can follow the conjunction operator.

Eventually: $\phi = \boxplus_{[a,b]} \phi$

Let $a_t^N = \min(t+1, N)$ and $b_t^N = \min(t+b, N)$, then define $\phi' = \bigvee_{a_t^N} \phi_i$, we have $r_t^\phi = r_t^{\phi'}$ and the encoding for the always operator can follow the disjunction operator.

Since we consider only the discrete time semantics of STL in this work, the advantage of this encoding is that it allows us to soften and harden the robustness constraints as necessary. For example, if the co-design problem is infeasible, we can allow $r_0^\phi > -\varepsilon$ for some $\varepsilon > 0$, thereby allowing a limited violation of the STL property during the co-design process, which enables the following iterative optimisation algorithm.

4.4 An iterative algorithm

When the design parameter vector θ , and controller gains K_1, K_2 are known, we consider the control synthesis problem as follows,

$$\max_{P_i, Q_i, P_s, U_i, V_s, R} r_0^\phi$$

Subject to the constraints,

$$\begin{cases} \bar{\Xi}_i(r_t^{\phi_i}) + X_i \Sigma_t + \Sigma_t^T X^T < 0, \\ \bar{\Xi}_s + X_s \Sigma_{s,t} + \Sigma_{s,t}^T X_s^T < 0, \\ \text{Temporal domain constraints based on (49)} \end{cases} \quad (50)$$

where $\bar{\Xi}_i(r_t^{\phi_i}) = \begin{bmatrix} \hat{\Xi}_i(r_t^{\phi_i}) & 0 \\ 0 & 0 \end{bmatrix}$ and $\hat{\Xi}_i(r_t^{\phi_i}) = \text{diag}(\Phi \otimes P_i + \Psi \otimes Q_i, \text{diag}\{\mathbf{I}, -\eta^2 \mathbf{I} + r_t^{\phi_i}\})$ or $\hat{\Xi}_i(r_t^{\phi_i}) = \text{diag}(\Phi \otimes P_i + \Psi \otimes Q_i, \text{diag}\{-\mathbf{I}, \eta^2 \mathbf{I} + r_t^{\phi_i}\})$. The first constraint in (50) requires the system satisfies frequency domain specification defined by ϕ_i at time t . When there exists eventually operator in frequency domain specification, Lemma 4.4 is used to relax the conditions. For each time t and atomic formula ϕ_i , the variable $r_t^{\phi_i}$ is used to indicate the robustness of the system. The second

constraint in (50) requires the system is asymptotically stable. The third constraint requires the system satisfies the temporal domain specifications, which requires the sequence of $r_0^\phi, r_1^\phi, \dots$ satisfies some specified patterns.

Since the physical parameter vector θ , and controller gains K_1 , and K_2 are fixed, the constraints in (50) are mixed integer linear. Thus the above problem can be solved with SDP solvers. When $P_i, Q_i, P_s, K_1, K_2, K_s, U_i, V_s, R$ are known in Theorem 4.3, we define the physical parameter optimisation problem as,

$$\max_{\theta \in \Delta} r_0^\phi$$

Subject to the constraints,

$$\begin{cases} \bar{\Xi}_i(r_t^{\phi_i}) + X_i \Sigma_t + \Sigma_t^T X^T < 0, \\ \bar{\Xi}_s + X_s \Sigma_{s,t} + \Sigma_{s,t}^T X_s^T < 0, \\ \text{Temporal domain constraints based on (49)} \end{cases} \quad (51)$$

The constraints in (51) are mixed integer LMIs, thus the problem can be solved with SDP solvers. Algorithm 1 solves the co-design problem with an iterative algorithm, which finds the optimal robustness degree.

Line 2 initialises the matrices K_1, K_2 and physical parameter θ_0 . During the initialisation procedure, we first randomly generate some physical parameter vectors, then use the full-information controller initialisation algorithm in [17] to find the optimal $[K_1, K_2]$ for the generated physical parameter vectors. If a stable system has been reached, we get the $[K_1, K_2]$ and θ in Line 4. Line 6 solves the optimisation problem defined by constraints (50) to obtain matrices related to the controller. Line 7 updates matrices K_1, K_2 . Based on the proof of Theorem 4.3, when $K_1^{i+1} \leftarrow (R^i)^{-1} L^i C_y$, $K_2^{i+1} \leftarrow (R^i)^{-1} L^i D_y$, the satisfaction status of the system will not be changed with respect to the frequency domain specifications, and we can obtain the controller gain $K_s = (R^i)^{-1} L^i$. Line 8 solves the optimal physical parameters with constraints defined in (51). Line 6–11 will be repeated until a predefined round limitation T_1 has been reached, or the parameter r_0^ϕ does not change much.

Algorithm 1 Iterative Algorithm for Co-design

Input: Frequency domain specification φ , state space realisation base $W_l, l = 1, \dots, r$, parameter space Δ , threshold δ , iteration limit T_1 , initial count $j = 0$.

Output: Optimal controller gain K_s^* and design parameter vector ϑ^* .

- 1: **if** $j = 0$ **then**
 - 2: Initialize the full-information controller gain $[K_1^0, K_2^0]$, and the physical parameter vector ϑ_0 ;
 - 3: **else**
 - 4: $\vartheta_0 \leftarrow \vartheta_j, K_1^0 \leftarrow K_1^j, K_2^0 \leftarrow K_2^j$ and $j \leftarrow 0$
 - 5: **repeat**
 - 6: (*Control synthesis*) Solve the mixed integer LMI optimisation problem defined by constraints (50) to obtain $r_0^{\phi_j}$,
 - 7: (*Control policy improvement*) Set $K_1^{j+1} \leftarrow (R^j)^{-1} L^j C_y$, $K_2^{j+1} \leftarrow (R^j)^{-1} L^j D_y$, and $K_s^j \leftarrow (R^j)^{-1} L^j$;
 - 8: (*Physical design*) Solve the mixed integer LMI optimisation problem defined by constraints (51) to obtain $r_0^{\phi_j}$ and ϑ^* ,
 - 9: (*Physical design improvement*) Set $\theta_j \leftarrow \theta^*$;
 - 10: Set $j \leftarrow j + 1$;
 - 11: **until** $j > T_1$ or $|r_0^{\phi_j} - r_0^{\phi_{j-1}}|/r_0^{\phi_j} < \delta$.
-

5. Numerical example

In this section, we provide two examples to illustrate the proposed co-design method. Numerical results are computed by using CVS toolbox (Grant & Boyd, 2014).

5.1 Energy harvesting MEMS devices

Due to the ubiquitous presence of environmental motions that can be transformed into electrical power, harvesting kinetic energy from mechanical movements has raised intensive interests among scholars (Du et al., 2019; Huang et al., 2019). Piezoelectric MEMS have been proven to be an attractive technology for harvesting micro-power from ambient vibrations (Kim et al., 2012). The goal of the co-design for energy harvesting MEMS devices is to activate the resonant mode at some frequencies associated with the vibration frequencies, such that the devices can harvest the largest amount of energy. The energy harvesting system can be described by the model in (12) with parameters given by

$$A = \begin{bmatrix} 0 & 0 & 1 & 0 \\ 0 & 0 & 0 & 1 \\ -kt - \kappa & kt + \kappa & -ct - \zeta & 0 \\ kt + \kappa & -kt - \kappa & 0 & -ct - \zeta \end{bmatrix},$$

$$B = [0 \ 0 \ 0 \ 1.3]^T,$$

$$C = [0 \ 1 \ 0 \ 0], \quad B_u = [0 \ 0 \ 2 + 0.2t \ 0]^T$$

$$D = D_u = 0, \quad C_y = \begin{bmatrix} 0 & 1 & 0 & 0 \\ 0 & 0 & 1 & 0 \end{bmatrix}, \quad D_y = \begin{bmatrix} 0 \\ 0 \end{bmatrix}$$

where k, κ, c, ζ are the time-invariant physical design parameters that are related to the effective stiffness and effective damping coefficient, which should be designed. Moreover, B_u is a time-varying matrix. In this device, we assume $v(t) = 0$, i.e. the time does not affect the frequency domain specification, and we want the MEMS device to satisfy the following specifications,

$$\begin{aligned} \varphi_{eh} &= \varphi_{eh}^1 \wedge \varphi_{eh}^2 \wedge \varphi_{eh}^3 \\ \varphi_{eh}^1 &= \square_{[0,3]} \square_{[0.3,0.4]} (f(G_{cl}(e^{j\omega}, t), \Pi_1) < 0) \\ \varphi_{eh}^2 &= \square_{[0,0.2]} (f(G_{cl}(e^{j\omega}, t), \Pi_2) < 0) \\ \varphi_{eh}^3 &= \square_{[1,20]} (f(G_{cl}(e^{j\omega}, t), \Pi_3) < 0), \end{aligned} \quad (52)$$

where $\Pi_1 = \text{diag}(-\mathbf{I}, 64\mathbf{I})$ requires the amplitude should be larger than 8, $\Pi_2 = \text{diag}(\mathbf{I}, -25\mathbf{I})$ requires the amplitude should be smaller than 5, and $\Pi_3 = \text{diag}(\mathbf{I}, -9\mathbf{I})$ requires the amplitude should be smaller than 3. $\square_{[0,3]} \psi$ shows the device will satisfy ψ at time 0, 1, and 2, respectively. The specification φ_{eh}^1 requires the frequency response of the system should be always larger than 8 within frequency interval $[0.3, 0.4]$ rad/s to harvest more energy, the specification φ_{eh}^2 requires the frequency response of the system should be always smaller than 5 within frequency interval $[0, 0.2]$ rad/s, and the specification φ_{eh}^3 requires the frequency response of the system should be always smaller than 3 within frequency interval $[1, 20]$ rad/s, respectively. The specification defines the board energy harvesting band for the device.

Denote the transfer function from w to z as T_{zw} and the frequency temporal domain specification is defined in (52). To

Table 2. Optimal robustness obtained with different number of basis systems.

r	2	3	4	5	6
$\rho(G_{cl, \theta, K_s, \varphi_{eh}})$	0.011	0.025	0.023	0.032	0.015

apply Algorithm 1, δ is set as $\delta = 10^{-3}$, and T_1 is 10, respectively. Before we solve the co-design problem defined in Problem 3.1, we need to construct the set of basis system matrices W_i defined in (13) and the parameters set Δ defined in (14). Intuitively, the larger the number of basis system matrices r , the better the design will be, but larger r will increase the computational load. In order to find an acceptable number for r , we first generate 100 pairs of parameters for $[k_i, \kappa_i, c_i, \zeta_i]$, where $i = 1, 2, \dots, 100$. Note that here we set the other basis matrices are the same for W_i . Then, we construct the design set Δ for each choice of r randomly, whose size is 1000. When r is chosen, we select r pair of parameters from the generated parameters and construct a matrix, denoted as \mathbb{S}_r . Assume $\mathbb{S}_0 = [k', c']$, where $k', \kappa', c', \zeta' = \text{argmax Entropy}([k_i, \kappa_i, c_i, \zeta_i])$, $i = 1, 2, \dots, 100$, and $\text{Entropy}(\mathbb{S})$ denotes the entropy of matrix \mathbb{S} . Then \mathbb{S}_{r+1} can be constructed as

$$\mathbb{S}_{r+1} = [\mathbb{S}_r; k', \kappa', c', \zeta'] \quad (53)$$

where $\bar{k}, \bar{c} = \text{argmax}_i \text{Entropy}(\mathbb{S}_{r+1})$. We check the optimal robustness obtained for five choices of r and the results are shown in Table 2, which indicate that 3 basis system matrices are enough to obtain a good design. The selected basis system designs are

$$\begin{aligned} & \begin{bmatrix} k_1 & \kappa_1 & c_1 & \zeta_1 \\ k_2 & \kappa_2 & c_2 & \zeta_2 \\ k_3 & \kappa_3 & c_3 & \zeta_3 \end{bmatrix} \\ &= \begin{bmatrix} 18.24 & 20.01 & 0.02121 & 0.02102 \\ 33.12 & 1.132 & 0.004221 & 0.02002 \\ 1.421 & 40.12 & 0.2435 & 0.02231 \end{bmatrix}, \end{aligned} \quad (54)$$

At the beginning for the three chosen basis system, θ is set as $[0.3 \ 0.3 \ 0.4]$, and the initial controller gain is defined as follows

$$K_1 = [-0.1412 \quad -0.6725 \quad -0.4123 \quad -0.1362]. \quad (55)$$

Then Algorithm 1 is applied to find the controller gain K_s and θ^* . The algorithm terminates after 10 iterations of search, and the results are

$$\begin{aligned} K_s^* &= [-0.1378 \ 0.2737] \\ \theta^* &= [0.3747 \ 0.3747 \ 0.2505] \end{aligned}$$

Then the design system matrix is $W^* = \sum_1^3 \theta_i^* W_i$ based on (13) and we can get the optimal designed physical parameters as $[k^*, \kappa^*, c^*, \zeta^*] = [19.5674, 17.9708, 0.0705, 0.0209]$, denoting the stiffness and damping coefficient of the system.

Figure 3 shows the frequency response of the closed-loop system at time 0, 1, and 2, respectively. The results show that all three scenarios can reach a satisfactory control (positive robustness). Note that the specification φ_{eh} has nested operator terms, e.g. $\square_{[0,3]} \square_{[0.3,0.4]} (f(G_{cl}(e^{j\omega}, t), \Pi_1) < 0)$, which means

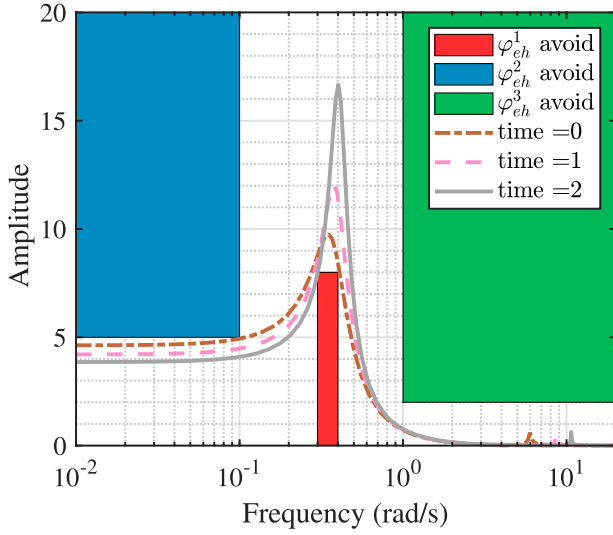


Figure 3. Frequency responses of the closed-loop system at different time.

the specification requires the frequency response satisfies the specification at time 0, 1, and 2, respectively. Moreover, specification without a nested operator requires the frequency domain specification is satisfied for all the time.

In order to investigate the advantage of the co-design approach, we conducted three comparison experiments. In the first experiment, we used the initialised physical and controller parameters directly and check the frequency response (we call this scenario ‘no design’). In the second experiment, we fixed the physical parameters to $\theta = [0.3, 0.3, 0.4]$ and found an optimal controller gain (we call this scenario ‘fixed-physical-system-optimal-controller design’), in which only Line 6 to 7 in Algorithm 1 was applied. In the third experiment, we fixed the controller gain and found the optimal physical parameters for θ (we call this scenario ‘fixed-controller-optimal-physical-system design’), in which only Line 8 in Algorithm 1 was applied. To illustrate the generality of the approach, we also conduct an experiment for the co-design scenario, in which we randomly initialise the physical parameter θ , then find the optimal design for both θ^* and K_s^* .

Figure 4 shows the frequency response of the device when $t = 0$ for the four experiment results, which show the ‘co-design’ approach can obtain the maximal robustness degree and satisfy the frequency domain specification. In contrast, the other three scenarios cannot reach a satisfactory design. Note that the results for these three scenarios depending on the initial parameters. If the parameters for the ‘fixed design’, ‘fixed controller’, and ‘no design’ cases are good, these scenarios will find designs to satisfy the specification, and they may reach the optimal designs if the initial parameters are optimal.

5.2 Logic MEMS devices

MEMS devices can be modelled as mass-spring systems. The mass-spring system used in this paper, modified from the system in Li and Gao (2014), is described by the model in (12). The results in Section 5.1 show that 2 basis system matrices can obtain a positive robustness degree. Therefore we use 2 basis system matrices in this case to simplify the presentation and the

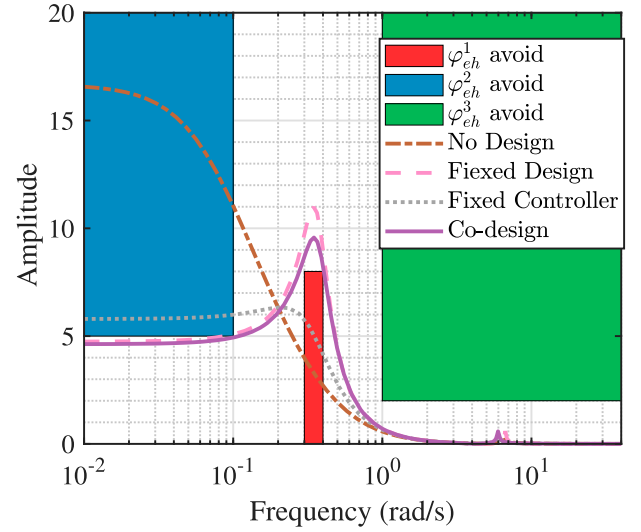


Figure 4. Frequency responses of four different design scenarios for the energy harvester at time 1: design with initialised parameters, fixed-physical-system-optimal-controller design, fixed-controller-optimal-physical-system design, and co-design.

basis system matrices are given as follows.

$$A_{1/2} = \begin{bmatrix} 0/0 & 0/0 & 1/1 & 0/0 \\ 0/0 & 0/0 & 0/0 & 1/1 \\ -20/-3 & 20/3 & -0.06/-0.2 & 0/0 \\ 20/3 & -20/-3 & 0/0 & -0.06/-0.2 \end{bmatrix},$$

$$B_{1/2} = [0/0 \ 0/0 \ 0/0 \ 1.3/1.2]^T,$$

$$C_{1/2} = [0/0 \ 1/1 \ 0/0 \ 0/0],$$

$$B_{u,1/2} = [0/0 \ 0/0 \ 0.3t + 1/0.12t + 0.8 \ 0/0]^T,$$

$$D_{1/2} = D_{u,1/2} = 0/0, \quad C_{y,1/2} = \begin{bmatrix} 0/0 & 1/1 & 0/0 & 0/0 \\ 0/0 & 0/0 & 1/1 & 0/0 \end{bmatrix},$$

$$D_{y,1/2} = [0/0 \ 0/0]^T$$

where indices of the matrices subscripts 1/2 denote the first or second basis system matrices.

Assume we want the MEMS device to realise a sequence of logic operations by exciting the device with specific AC signals. For example, if we want the device to realise NOR, XOR, AND gate sequentially, then the frequency domain specifications, φ_{mems} , is defined in (5.2).

$$\varphi_{mems} = \square_{[0,3]}(\varphi_1 \wedge \varphi_2 \wedge \varphi_3)$$

$$\varphi_1 = \diamond_{[v(t), 0.1+v(t)]}(f(G(e^{j\omega}, t), \Pi_1) < 0)$$

$$\varphi_2 = \square_{[1,100]}(f(G(e^{j\omega}, t), \Pi_2) < 0)$$

$$\varphi_3 = \square_{[0,0.3]}(f(G(e^{j\omega}, t), \Pi_2) < 0),$$

where $G(e^{j\omega}, t)$ is the frequency response of the MEMS device, $\Pi_1 = \text{diag}(\mathbf{I}, -225\mathbf{I})$ requires the amplitude should be larger than 15, $\Pi_2 = \text{diag}(\mathbf{I}, -25\mathbf{I})$ requires the amplitude should be smaller than 5; $\diamond_{[v(t), 0.1+v(t)]}$ indicates the frequency interval, where $v(t) = 0.1t + 0.4$, and φ_1 shows the device will be eventually activated to a high output with activation frequencies

between $v(t)$ and $0.1 + v(t)$ rad/s; φ_2 and φ_3 shows the device will output low voltages when the activation frequencies are out of $[v(t), 0.1 + v(t)]$, $\square_{[0,3]}$ indicates at time t , B_u will be changed according to the parametric varying function.

Denote the transfer function from w to z as T_{zw} . To apply Algorithm 1, δ is set as $\delta = 10^{-3}$, T_1 and T_2 are set as 15 and 10, respectively. Moreover, since $D_{y,1}$, $D_{y,2}$ are zero, matrix K_2 in the initial control gain can be set to zero, reducing to a static output feedback controller.

At the beginning, θ is set as $[0.5, 0.5]$, and the initial controller gain is defined as follows

$$K_1 = [-0.1415 \quad -0.3513 \quad -0.2242 \quad -0.2322]. \quad (56)$$

Then Algorithm 1 is applied to find the optimal controller gain K_s^* and physical system design θ^* . The algorithm terminates after 10 iterations of binary search and the results are

$$K_s^* = [-0.5325 \quad 0.1241], \quad \theta^* = [0.5560 \quad 0.4440]. \quad (57)$$

Then the optimal design for the device is

$$A = \begin{bmatrix} 0 & 0 & 1 & 0 \\ 0 & 0 & 0 & 1 \\ -12.45 & 12.45 & -0.1666 & 0 \\ 12.45 & -12.45 & 0 & -0.1666 \end{bmatrix},$$

$$B = [0 \quad 0 \quad 0 \quad 1.290]^T,$$

$$C = [0 \quad 1 \quad 0 \quad 0], \quad B_u = [0 \quad 0 \quad 0.2201t + 0.9112 \quad 0]^T,$$

$$C_y = \begin{bmatrix} 0 & 1 & 0 & 0 \\ 0 & 0 & 1 & 0 \end{bmatrix}, \quad D = D_u = 0, \quad D_y = [0 \quad 0]^T$$

The frequency responses of the optimal design for different logic gates, which depicts the designed system can realise NOR, XOR, and AND gate when it is actuated with an AC signal with frequency at 0.45, 0.55, and 0.65 rad/s, respectively. During the logic operation, the bias tee will output the associated shift voltage, which sets the parameter to $\vartheta(0)$, $\vartheta(1)$, and $\vartheta(2)$, sequentially.

In order to investigate the advantage of the co-design approach, we also conducted three comparison experiments as in the energy harvesting MEMS design case. Figure 6 shows the robustness degree $\rho(G_{cl}, \theta, K_s, \varphi_{mems})$ obtained by the three design scenarios that needs Algorithm 1 (the first experiment did not need Algorithm 1) and the time costs with respect to the number of binary iterations used. Specifically, for the co-design scenario, we randomly initialise the physical parameter 10 times and calculate the mean robustness degree and its standard deviation. The results show that all the three scenarios can reach a satisfactory design (positive robustness), while the co-design approach can find a larger robustness degree with respect to the specifications, indicating that the co-design can find a better result. Figure 6 also shows the average time cost to reach an optimal results (the iteration limit is set to 4). However, the co-design algorithm takes twice the time to reach optimal robustness with respect to the fixed controller or fixed design case, the reason is that the co-design approach uses an alternately optimised way to find the optimal parameters, which solves a sequence of optimisation problems. The other

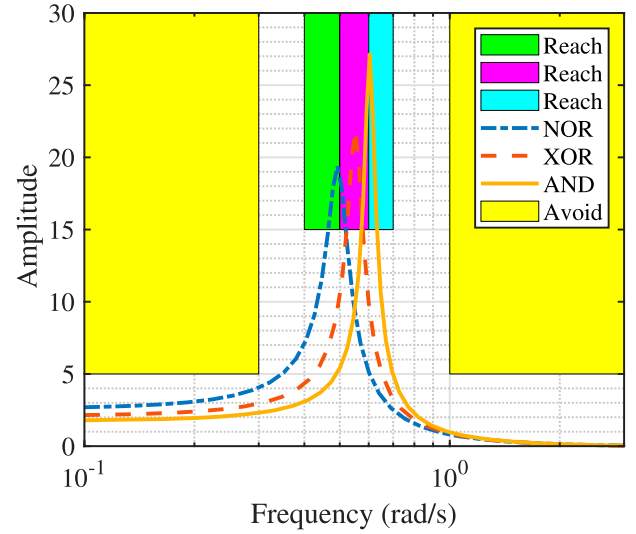


Figure 5. Frequency responses of device designed with the proposed co-design approach to realise 'NOR', 'XOR', and 'AND' gate, respectively.

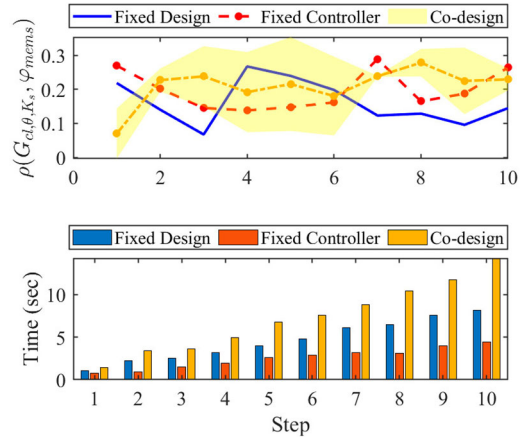


Figure 6. $\rho(G_{cl}, \theta, K_s, \varphi_{mems})$ and time costs with respect to different iteration limits T_1 for the three design scenarios shown in Figure 5.

two methods only need to solve one optimisation problem. The time costs show the setup time takes a large portion of the costs for the optimisation problem since the co-design problem only takes twice the time of the other two. Considering that the design procedure is conducted offline, this computational cost is acceptable. For the use case of cyber-physical systems co-design, the processing time is not critical (though it is reasonable, based on our experiments), and the proposed method is suitable when neither the fixed controller nor fixed design approaches yield a satisfactory design.

Figure 7 shows the frequency response of the device at 'NOR' gate for the four experiment results, which shows the 'co-design' approach can obtain the maximal robustness degree. The 'Fixed Design' and 'Fixed Controller' approaches can obtain positive robustness, which means the two approaches can find a satisfactory design. However, the 'No Design' approach cannot find a satisfactory design. The results show that 'co-design' has the advantage over the other approach, which is reasonable since the 'co-design' approach can optimise more design parameters than the others.

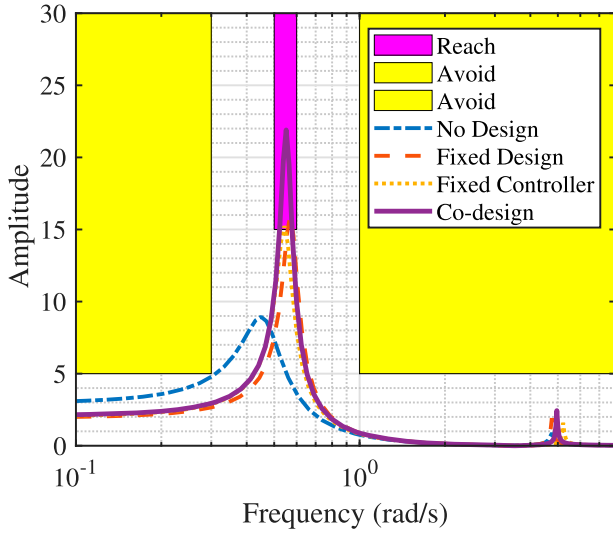


Figure 7. Frequency responses of four different design scenarios when the device performs logic XOR gate: design with initialised parameters, fixed-physical-system-optimal-controller design, fixed-controller-optimal-physical-system design, and co-design.

5.3 Discussions

It can be shown that the series $\{r_0^{\varphi,0}, r_0^{\varphi,1}, \dots\}$ generated by Algorithm 1 is non-decreasing. Therefore, it is expected that the satisfiable parameters can be found by Algorithm 1 with respect to an expected robustness degree if parameters exist. However, since the problem is non-convex, the initial parameters affect the search direction, and it is likely that the obtained parameters are only locally optimal. The contribution of Algorithm 1 in the current paper includes: First, we transfer the co-design problem into a sequence of SDP problems. Second, instead of solving the co-design problem for optimal robustness directly, we try to reach a value that is related to the robustness degree with an iterative algorithm. Note that the setting of $\Xi(r_t^{\varphi_i})$ in (50) and (51) makes the optimal $r_t^{\varphi_i} \neq \rho(\varphi_i, t)$, but the increase of $r_t^{\varphi_i}$ will lead to the increase of $\rho(\varphi_i, t)$ when $r_t^{\varphi_i}$ is positive. Therefore, the solution found by Algorithm 1 may not be the global optimal but it is a satisfiable solution.

The complexity of the solving the optimisation problem in (50) depends on the dimension of the LMI constrains. Assume the system dimension is defined in (12), the number of predicates in STL formula is κ , and the horizon of the temporal operator is N . Then the dimension complexity of the LMI is $\mathcal{O}(Nn_s\kappa + Nn_z\kappa + Nn_w\kappa)$, where n_s, n_z and n_w are the dimensions of the system defined in (12).

In this paper, static output feedback controller is used, which has been widely used (Cheng et al., 2019, 2021), since it is easy to implement. However, when the specifications are more complex than the numerical examples, it is possible that there exists no state output-feedback controller that can satisfy the spectral temporal logic. To address this issue, a parameter-varying state output-feedback controller can be used, in which the control input can be described as $u(t) = K_s(\vartheta(t))y(t)$. Moreover, Algorithm 1 can also be used to find the optimal parameter-varying state output-feedback controller, in which the matrices K_1, K_2, L, R are parameter-varying, i.e. each time will have an

independent pair of K_1, K_2, L, R . Additionally, in many application scenarios, we do care about the physical parameter varying process with given spectral temporal specifications, in which the proposed method can be used to find the optimal physical parameters at each time with known controller. For example, in fault detection applications for machinery systems, the spectral temporal specifications can be found with data-driven method (Chen et al., 2020), the proposed method can be used to identify the physical parameters, thus detecting the current state of the system.

Even though there exist other controllers for the ‘co-design’ problem, there exists no algorithm for the ‘co-design’ with respect to complex frequency temporal domain specifications that can be described with spectral temporal logic. In the control community, existing ‘co-design’ algorithms can only deal with simple frequency domain specifications. Moreover, in this paper, we propose a new formal language for spectral temporal domain specifications and provide the conditions to satisfy the specification in the form of mixed integer linear matrix inequality. Other types of controllers may achieve good performance in terms of specification satisfaction, but the proposed method can transform the ‘co-design’ problem into semi-definite programming problems, which can be solved with existing solvers efficiently. In other words, we formulate the ‘co-design’ problem formally, including the complex spectral temporal domain specifications, and transform it into a problem that can be solved with mature tools. Basically, this paper solves an optimisation problem with non-linear constraints in the form of matrix inequalities. Until now, there is no traditional optimisation algorithm that can deal with these non-linear constraints. For example, the genetic algorithm (GA) and particle swarm optimisation (PSO) method embedded in Matlab cannot deal with the non-linear matrix inequalities, in which GA can only handle linear matrix inequalities and PSO can only add lower and upper bounds to the variables. Therefore, one of the contributions of this paper is that we decompose the ‘co-design’ problem with non-linear constraints into a sequence of optimisation problems with linear constraints in the form of linear matrix inequalities, such that traditional optimisation algorithms, e.g. the GA, can be applied to solve the decomposed problems. In this paper, the tool CVS toolbox (Grant & Boyd, 2014) with a mature solver, called Gurobi, was used to solve the decomposed problem. Since the contribution of this paper does not focus on solving of the decomposed problems, we did not compare the performance of different solvers, but the readers can try different solvers by themselves for their interests.

6. Conclusions

This paper solves a co-design problem for LPV systems with spectral temporal domain specifications for MEMS devices. Static output feedback controllers and physical system parameters are designed, with spectral temporal logic describing high-level complex specifications. Theoretical results show the constraints of the STL formula can be transformed into matrices inequalities and equalities. To solve the co-design problem with non-linear constraints, an iterative algorithm is developed, which finds a satisfiable solution for the problem subject to spectral temporal logic formula. The numerical examples show that

the proposed algorithm can achieve good performance for the co-design of LPV systems.

Disclosure statement

No potential conflict of interest was reported by the author(s).

Funding

This work is partially supported by the National Key R&D Program of China [grant number 2021YFB3301402], partially supported by the National Natural Science Foundation of China [grant number 52305105], the Basic and Applied Basic Research Foundation of Guangdong Province [grant numbers 2022A1515240027 and 2023A1515010812], the Basic and Applied Basic Research Foundation of Guangzhou [grant number 2023A04J1582].

References

- Allison, J. T., Guo, T., & Han, Z. (2014). Co-design of an active suspension using simultaneous dynamic optimization. *Journal of Mechanical Design*, 136(8), 081003. <https://doi.org/10.1115/1.4027335>
- Balram, K. C., & Srinivasan, K. (2022). Piezoelectric optomechanical approaches for efficient quantum microwave-to-optical signal transduction: The need for co-design. *Advanced Quantum Technologies*, 5, 2100095. <https://doi.org/10.1002/qute.v5.3>
- Chanekar, P. V., Chopra, N., & Azarm, S. (2016). A new formulation for co-design of linear systems with system matrices having affine design variables. In *Indian Control Conference* (pp. 507–513). IEEE.
- Chanekar, P. V., Chopra, N., & Azarm, S. (2018). Co-design of linear systems using generalized benders decomposition. *Automatica*, 89, 180–193. <https://doi.org/10.1016/j.automatica.2017.12.009>
- Chappanda, K., Ilyas, S., & Younis, M. I. (2018). Micro-mechanical resonators for dynamically reconfigurable reduced voltage logic gates. *Journal of Micromechanics and Microengineering*, 28(5), 055009. <https://doi.org/10.1088/1361-6439/aaafe5>
- Chen, G., Sabato, Z., & Kong, Z. (2018). Formal interpretation of cyber-physical system performance with temporal logic. *Cyber-Physical Systems*, 4(3), 175–203. <https://doi.org/10.1080/23335777.2018.1510857>
- Chen, G., Wei, P., Jiang, H., & Liu, M. (2020). Formal language generation for fault diagnosis with spectral logic via adversarial training. *IEEE Transactions on Industrial Informatics*, 18(1), 119–129. <https://doi.org/10.1109/TII.2020.3040743>
- Cheng, J., Park, J. H., Zhao, X., Cao, J., & Qi, W. (2019). Static output feedback control of switched systems with quantization: A nonhomogeneous sojourn probability approach. *International Journal of Robust and Nonlinear Control*, 29(17), 5992–6005. <https://doi.org/10.1002/rnc.v29.17>
- Cheng, J., Wang, Y., Park, J. H., Cao, J., & Shi, K. (2021). Static output feedback quantized control for fuzzy Markovian switching singularly perturbed systems with deception attacks. *IEEE Transactions on Fuzzy Systems*, 30(4), 1036–1047. <https://doi.org/10.1109/TFUZZ.2021.3052104>
- Chiu, W.-Y. (2017). Method of reduction of variables for bilinear matrix inequality problems in system and control designs. *IEEE Transactions on Systems, Man, and Cybernetics: Systems*, 47(7), 1241–1256. <https://doi.org/10.1109/TSMC.2016.2571323>
- Donzé, A., & Maler, O. (2010). Robust satisfaction of temporal logic over real-valued signals. In *International Conference on Formal Modeling and Analysis of Timed Systems* (pp. 92–106). Springer.
- Du, S., Jia, Y., Zhao, C., Amaratunga, G. A., & Seshia, A. A. (2019). A nail-size piezoelectric energy harvesting system integrating a MEMS transducer and a CMOS SSHI circuit. *IEEE Sensors Journal*, 20(1), 277–285. <https://doi.org/10.1109/JSEN.7361>
- Ghayesh, M. H., Farokhi, H., & Amabili, M. (2013). Nonlinear behaviour of electrically actuated MEMS resonators. *International Journal of Engineering Science*, 71, 137–155. <https://doi.org/10.1016/j.ijengsci.2013.05.006>
- Grant, M., & Boyd, S. (2014). CVX: Matlab software for disciplined convex programming, version 2.1. <https://cvxr.com/cvx>.
- Huang, M., Hou, C., Li, Y., Liu, H., Wang, F., Chen, T., Yang, Z., Tang, G., & Sun, L. (2019). A low-frequency MEMS piezoelectric energy harvesting system based on frequency up-conversion mechanism. *Micromachines*, 10(10), 639. <https://doi.org/10.3390/mi10100639>
- Ilyas, S., Jaber, N., & Younis, M. I. (2017a). MEMS logic using mixed-frequency excitation. *Journal of Microelectromechanical Systems*, 26(5), 1140–1146. <https://doi.org/10.1109/JMEMS.2017.2712859>
- Ilyas, S., Jaber, N., & Younis, M. I. (2017b). Multi-function and cascaded MEMS logic device. In *2017 IEEE 30th International Conference on Micro Electro Mechanical Systems* (pp. 877–880). IEEE.
- Iwasaki, T., & Hara, S. (2005). Generalized KYP lemma: Unified frequency domain inequalities with design applications. *IEEE Transactions on Automatic Control*, 50(1), 41–59. <https://doi.org/10.1109/TAC.2004.840475>
- Karami, M. A., & Moez, K. (2019). Systematic co-design of matching networks and rectifiers for CMOS radio frequency energy harvesters. *IEEE Transactions on Circuits and Systems I: Regular Papers*, 66(8), 3238–3251. <https://doi.org/10.1109/TCSI.8919>
- Kim, B., Hopcroft, M. A., Candler, R. N., Jha, C. M., Agarwal, M., Melamud, R., Chandorkar, S. A., Yama, G., & Kenny, T. W. (2008). Temperature dependence of quality factor in MEMS resonators. *Journal of Microelectromechanical Systems*, 17(3), 755–766. <https://doi.org/10.1109/JMEMS.2008.924253>
- Kim, S.-G., Priya, S., & Kanno, I. (2012). Piezoelectric MEMS for energy harvesting. *MRS Bulletin*, 37(11), 1039–1050. <https://doi.org/10.1557/mrs.2012.275>
- Li, X., & Gao, H. (2014). A heuristic approach to static output-feedback controller synthesis with restricted frequency-domain specifications. *IEEE Transactions on Automatic Control*, 59(4), 1008–1014. <https://doi.org/10.1109/TAC.2013.2281472>
- Maler, O., & Nickovic, D. (2004). Monitoring temporal properties of continuous signals. In Y. Lakhnech & S. Yovine (Eds.), *Formal techniques, modelling and analysis of timed and fault-tolerant systems* (pp. 152–166). Springer.
- Raman, V., Donzé, A., Maasoumy, M., Murray, R. M., Sangiovanni-Vincentelli, A., & Seshia, S. A. (2014). Model predictive control with signal temporal logic specifications. In *53rd IEEE Conference on Decision and Control* (pp. 81–87). IEEE.
- Rizzon, L., & Passerone, R. (2016). Cyber/physical co-design in practice: Case studies in metroii. In *11th IEEE Symposium on Industrial Embedded Systems (SIES)* (pp. 1–10). IEEE.
- Silvas, E., Hofman, T., Murgovski, N., Etman, L. P., & Steinbuch, M. (2017). Review of optimization strategies for system-level design in hybrid electric vehicles. *IEEE Transactions on Vehicular Technology*, 66(1), 57–70.
- Skelton, R. (1989). Model error concepts in control design. *International Journal of Control*, 49(5), 1725–1753. <https://doi.org/10.1080/00207178908559735>
- Zhong, Z., Xu, C., Billian, B. J., Zhang, L., Tsai, S.-J., Conners, R. W., Centeno, V. A., Phadke, A. G., & Liu, Y. (2005). Power system frequency monitoring network implementation. *IEEE Transactions on Power Systems*, 20(4), 1914–1921. <https://doi.org/10.1109/TPWRS.2005.857386>